

Research papers

An analytical method for sizing energy storage in microgrid systems to maximize renewable consumption and minimize unused storage capacity

Han Kun Ren^{*}, Masaō Ashtine, Malcolm McCulloch, David Wallom

Department of Engineering Science, University of Oxford, Oxford, OX1 3PJ, UK

ARTICLE INFO

Keywords:

Renewable energy system
Battery energy storage
Optimal sizing
Microgrid
Solar PV

ABSTRACT

This paper presents a novel analytical method to optimally size energy storage in microgrid systems. The method has fast calculation speeds, calculates the exact optimal, and handles non-linear models. The method first constructs a temporal storage profile of stored energy, based on how storage charges and discharges in response to renewable generation and load demand. The storage is sized according to the largest cumulative charge or discharge in the profile. In essence, the storage profile represents how storage is utilized within a given system, and the method sizes optimal storage to maximize that profile, such that storage utilization is maximized, and unutilized or wasted storage is eliminated. Maximizing storage utilization also maximizes renewable consumption and minimizes load shedding, as storage utilization is the temporal transfer of energy from renewable generation to load demand. The proposed method is extended iteratively to account for storage's energy limits, power limits, and energy leakage. Two solar–battery case studies demonstrate the method. The first study shows that optimally sized storage does not have wasted capacity due to over-sizing, nor cause energy deficits due to under-sizing. The second case study shows increasing the storage size reduces the marginal increase in energy provided by storage, indicating diminishing returns. The diminishing return thresholds are defined by the largest daily and annual storage designs. The result shows the largest daily design only requires 3% of the annual design's storage size, but provides 80% of the energy provided by the annual design. The proposed method can be used as a decision support tool for energy analysts, to determine required storage capacity when coupled with known renewable generation and load demand.

1. Introduction

The paper presents a novel analytical method to optimally size energy storage. The method is fast, calculates the exact optimal, and handles non-linear models. The need for storage sizing arises from the rising greenhouse gas emissions, which are considered the main culprit of climate change. Many countries have signed the Paris Agreement to curb emissions and become carbon neutral by 2050 [1]. However, currently more than 73% of global greenhouse gas emissions come from the energy sector, which relies on fossil fuels [2]. Renewable generations, such as solar and wind, produce no emissions during operation, and have lower life-cycle emissions than fossil fuel power plants [3]. Moreover, solar farms produce electricity significantly cheaper than fossil fuel power plants in many countries [4]. However, renewables are weather-dependent, causing their generation to be intermittent and non-dispatchable. The intermittency is dangerous for the stability of the electrical system, and the lack of dispatchability creates mismatches between electricity generation and demand, resulting in curtailed generations and unmet demands. Energy storage can mitigate renewable

intermittency and non-dispatchability. Storage regulates intermittency by storing energy during high generation periods, then releasing that energy to supplement low generation periods. In the same manner, storage can charge from surplus generation and discharge to meet the excess demand, effectively providing dispatchability to renewables. Proper sizing ensures storage has enough capacity to charge and discharge energy when required, and achieves this without unutilized or wasted storage. There are four main approaches to size energy storage: enumerative, mathematical programming, meta-heuristic and analytical.

1.1. Enumerative approach

The enumerative approach systematically goes through a defined range of storage sizes, simulates the storage behavior at each size, and then selects the best-performing size [5]. Yang et al. used an enumerative method to size solar photovoltaics (PV), wind turbines, and battery banks for a telecommunication relay station [6]. The method

^{*} Corresponding author.

E-mail address: han.ren@eng.ox.ac.uk (H.K. Ren).

<https://doi.org/10.1016/j.est.2023.107735>

Received 30 January 2023; Received in revised form 4 May 2023; Accepted 15 May 2023

Available online 1 June 2023

2352-152X/© 2023 The Author(s). Published by Elsevier Ltd. This is an open access article under the CC BY-NC-ND license (<http://creativecommons.org/licenses/by-nc-nd/4.0/>).

Nomenclature

α	Multiplier
Δt	Change in time (hour)
ϵ	Permissible difference limit
η_c	Charge efficiency
η_d	Discharge efficiency
ϕ	Degradation factor
σ	Storage energy leakage rate (%/hour)
C	Critical point matrix
D	Difference matrix
L	Lower triangular matrix
C_c	Charge C-rating
C_d	Discharge C-rating
D	Demand power (kW)
DoD	Depth of discharge (%)
E	Storage size (kWh)
E_{tot}	Storage's total energy capacity (kWh)
G	Generation power (kW)
N	Storage cycle life (cycle)
P_c	Maximum charge rate (kW)
P_d	Maximum discharge rate (kW)
Q	Annual energy throughput (kWh/year)
r_n	Randomized data of normal distribution
r_u	Randomized data of uniform distribution
S	Storage energy level (kWh)
s	Standard deviation
S_s	Sustainable starting storage level (kWh)
S_{low}	Lower storage energy limit (kWh)
S_{up}	Upper storage energy limit (kWh)
T	Time at the end of the design period (hour)
t	Time in the first design period (hour)
t'	Time in the second design period (hour)
t_n	Time at the n th critical point (hour)
T_{cal}	Storage calendar life (year)
T_{life}	Storage lifespan (year)
x	Historical data
\bar{x}	Mean value

iterates through ranges of solar, wind, and battery capacities. At each iteration, the system is simulated, and the occurrence of unmet demand is calculated in terms of Loss of Power Supply Probability (LPSP). The cost for system sizes meeting a specific LPSP is calculated, and the lowest cost system size is selected. Borowy proposed a hybridized enumerative and analytical method to size solar PV with batteries [7]. The enumerative method iterates through solar and battery capacity ranges, and calculates the LPSP. An analytical equation models the solar and battery capacities relationship at a specific LPSP. The analytical equation is solved with a cost equation to yield the lowest cost sizing. Similar to Borowy's approach, Jakhrani et al. also used an enumerative-analytical method to size solar-battery systems [8]. Cabral et al. used a probabilistic-enumerative method to size a solar-battery system [9]. The study found the addition of the probabilistic method yielded a smaller storage size with acceptable LPSP. Similarly, Zhu et al. also used a probabilistic-enumerative method to size a solar-battery system [10]. The study sized storage to reduce solar power back-feeding the grid. Bartolucci et al. used the enumerative method to size battery and fuel-cell with solar generation [11]. The study found that battery is more economical than fuel-cell when coupled with solar generation. Furthermore, the study showed increasing battery size has a diminishing return on battery energy provided to the system. Zhang

et al. used the enumerative method to size a grid-connected solar-battery system [12]. The study found that sizing to maximize renewable consumption will result in a lower initial investment, but a longer payback period. The Hybrid Optimization of Multiple Energy Resources (HOMER) software sizes hybrid renewables using the enumerative approach. Ma et al. used HOMER to assess the feasibility of a solar-wind-battery system for a remote island [13]. The study found that the island's existing diesel power system can be fully replaced by the renewable system. Halabi et al. used HOMER to size a solar-diesel-battery system for a village [14]. The study found that battery is mainly used as backup power due to the higher cost.

1.2. Mathematical programming approach

The mathematical programming approach contains classical optimization algorithms, such as linear programming and gradient descent algorithms [15]. The algorithms optimize storage size based on objective and constraint equations describing the energy system. Generally, there are four core constraints [16]. The first constraint says the future storage level is equal to the current storage level plus the change in stored energy due to charge or discharge. The second constraint says charge and discharge rates must be within the storage's power limits. The third constraint says storage levels must be within the storage's energy limits. The final constraint says storage levels at the start and end of the design period must be equal [17]. Chen et al. used mixed-integer linear programming to size storage [18]. The method first calculates the minimum storage size via the minimum of the total charged or discharged energy. The minimum size forms a part of the constraints, which are fed into mixed-integer linear programming to calculate the storage size. Nick et al. utilized mixed-integer second-order cone programming to size storage in a distribution network [19]. The goal is to minimize the storage cost and the network operation cost. The study accounts for the growth in load, PV capacity, and fuel cost. The study found that optimally sized and placed storage can reduce the total system cost. Atia and Yamada used the probabilistic approach with mixed-integer linear programming to size a grid-connected solar-wind-battery system [20]. The study used normal distribution to model solar generation and demand, and Weibull distribution to model wind generation. The study found storage can generate more profit with highly varied electricity pricing, and demand flexibility can reduce the storage requirement. Al-Ghussain et al. used the generalized reduced gradient algorithm to size hydrogen fuel cell and pumped hydro in a solar-wind-storage system [21]. The study found hydrogen fuel cells can fill the power gap when pumped hydro is starting up, which increases renewable consumption. Opathella et al. used mixed integer linear programming to size energy storage and conventional generator [22]. The objective was to minimize the storage, generator, and grid electricity import costs. The study optimized the investment schedule for each storage and generator. The study found energy storage can improve grid flexibility and reliability, which reduces the total system cost. Pena et al. used mixed integer linear programming to size battery storage with conventional generators and hydro-power [23]. The objective was to minimize battery cost and system operation costs. The study found that increasing battery size reduces conventional generator dispatches and the overall cost.

1.3. Meta-heuristic approach

The meta-heuristic approach contains modern optimization algorithms, such as genetic and particle swarm algorithms [24]. Meta-heuristic algorithms smartly navigate the size search space, enabling faster convergence to near-optimal sizing. In a later paper by Yang et al., the solar-wind-battery sizing method is improved with genetic algorithm and more accurate models. [25]. The new method is benchmarked against the real system, and found the sized storage could support the demand. Zhang et al. also used genetic algorithm to size

a grid-connected solar–battery system [26]. The study proposed three operation strategies: conventional, demand shifting, and a hybrid of conventional and peak-shaving. The hybrid strategy performed the best in terms of cost and self-sufficiency. In another study by Zhang et al., hydrogen and battery storage are compared in a solar–storage system [27]. The study found that the battery system is cheaper while the hydrogen system provides higher power quality. Shabani et al. used genetic algorithm to size a solar–wind–storage system [28]. The study found combining wind and solar generations reduces storage size requirements. Lai et al. used seven mathematical programming methods to size an anaerobic digestion plant with solar and storage [29]. The study found the most suitable algorithm is particle swarm optimization with interior point method. Maleki et al. utilized the probabilistic Monte Carlo simulation with particle swarm algorithm to size a solar–wind–battery system [30]. The Monte Carlo simulation generates a distribution of storage sizes, and the final sizing is selected based on the distribution's mean value. The study found wind–battery system has the lowest cost, due to the lower storage requirement. Falama et al. used the firefly algorithm to size battery and hydrogen storage with solar generation [31]. The objective is to minimize the cost of energy and LPSP. The study found the solar–battery system is more economically profitable, as the current cost of hydrogen fuel cells is too high. Fares et al. compared ten meta-heuristic algorithms for sizing storage in a solar–wind–battery system [32]. The study found that simulated annealing has the best compromise between accuracy and speed. Ghaffari et al. used the crow search algorithm to size storage in a solar–wind–battery system [33]. The study found optimal sizing and placement of storage can reduce power loss and fluctuation. Saini and Gidwani used genetic algorithm to size a solar–battery system [34]. The study found optimal sizing and placement of storage can reduce over-voltage, power loss, and increase solar PV penetration.

1.4. Analytical approach

The analytical approach uses storage models to construct the storage energy profile, and then sizes the storage based on the profile [35]. Cao et al. proposed an analytical method to size batteries for smoothing wind power output [36]. The method first constructs the storage level profile. Then, storage is sized according to the difference between the initial and the maximum change in storage level. Boonluk et al. proposed an analytical storage sizing method to improve the power quality in networks [37]. The method sizes storage according to the difference between the maximum and minimum storage levels. Gu et al. proposed an analytical method for sizing storage in a solar–wind–battery system [38]. The method sizes storage according to the maximum change in storage level during the design period. Neto et al. proposed an analytical-probabilistic method to size dual battery storage systems [39]. The method uses a probabilistic model to calculate the distribution of energy and power deficits. The storage is then sized based on the deficits. The storage operation is optimized, where the smaller secondary battery is operated to reduce the degradation of the primary battery. The battery degradation is modeled using the Schiffer model. The study found optimal sizing and operation of the dual battery setup extended the primary battery's useful life, and reduced the system cost. Arun et al. proposed an analytical method to size storage in a solar–diesel–battery system [40]. The storage profile is constrained to positive values, and the starting and ending storage levels must be equal. Then, storage is sized according to the highest storage level in the profile. Norbu and Bandyopadhyay also used Arun's storage sizing method to reduce unmet demands [41]. Bandyopadhyay improved Arun's method by shifting the storage profile to meet the constraints [42]. First, the storage profile is shifted upwards to eliminate negative values. Then, the latter section of the profile is shifted downward to ensure equal starting and ending storage levels. The storage is sized according to the highest storage level in the shifted profile. Similarly, Nassar et al. proposed shifting the storage profile

upwards iteratively, such that the final profile has no negative energy values [43]. The storage is then sized according to the final storage profile's highest storage level. Kichou et al. proposed a similar method, where the difference between the starting storage level and the lowest storage level is used to size storage [44]. Data collected from the built storage system shows the discrepancy between real and simulated storage size is less than 5%. Moreover, the study found data resolution of less than one hour has minimal effect on the accuracy of storage sizing. In a previous paper by the author, a preliminary version of the proposed method is applied to size a solar–storage system [45]. The analytical method sizes storage and solar to define the size search space. Then the enumerative method iterates through the search space to find the lowest cost system size. The sizing process is repeated with projected future costs, and the study found solar and storage will make up greater portions of the energy system as their costs come down.

1.5. Research gap

The enumerative approach systematically iterates through storage sizes in a defined search range, simulates the storage behavior at each size, then selects the best-performing size. This approach has two major drawbacks. First, it can be calculation-intensive and time-consuming. Second, the approach cannot find the optimal size outside the defined search range. The meta-heuristic approach can mitigate the two drawbacks of the enumerative approach. However, meta-heuristic algorithms are still comparatively slow, and cannot guarantee optimal solutions due to their stochastic nature. Unlike meta-heuristic algorithms, some classical optimization algorithms are fast and can guarantee optimal. However, they require linear approximation when applied to systems with non-linear models. The analytical approach can handle non-linear models, guarantees exact optimal, and is the fastest approach.

Currently, few analytical methods have been developed for sizing energy storage, and they cannot be universally applied. Some analytical methods can fail with erratic storage profiles, while others do not produce the optimal sizing. Most analytical methods are only designed for energy systems with over-generation, thus they cannot be applied to other systems. Moreover, most analytical methods do not account for storage energy leakage, which can affect long-term storage sizing. Some analytical methods do not account for storage power limits, which yield storage designs with unrealistic power requirements. Some analytical methods do not require equal starting and ending storage levels, which means the storage profile is not repeatable for future periods. The lack of repeatability means the storage size is only valid for the current design period, but not for future periods.

1.6. Contribution

The paper presents a novel analytical method for sizing energy storage, addressing the aforementioned issues. The proposed method can be applied to all storage profiles, accounting for storage's energy limits, power limits, and energy leakage. Moreover, the sized storage will have equal starting and ending storage levels, ensuring the sizing's validity for future periods. The proposed method focuses on the technical aspects of storage sizing. The sizing is not affected by economic variability, and will always yield the storage size that maximizes storage utilization while eliminating wasted storage capacity. However, for readers interested in implementing this sizing algorithm in a techno-economic setting, please refer to a previous paper by the author: [45]. Major contributions made in this paper are as follows:

- The proposed sizing algorithm is built on a new theory that storage should be sized according to the largest cumulative charge or discharge it can experience.
- Compared to other popular storage sizing methods, the proposed method has a fast calculation speed, calculates the exact optimal, and can handle non-linear models, as summarized in Table 1.

Table 1
Comparison of storage sizing methods.

	Proposed	Mathematical	Meta-heuristic	Enumerative
Fast Speed	✓	✓	X	X
Exact Optimal	✓	✓	X	X
Non-linear Model	✓	X	✓	✓

- The proposed method yields the optimal storage size that maximizes storage utilization while eliminating unutilized storage capacity. Maximizing storage utilization also maximizes renewable consumption and minimizes load shedding, as storage utilization is the temporal transfer of energy from renewable generation to load demand.
- The method is extended iteratively to account for depth of discharge, maximum charge and discharge rates, and storage leakage. Storage leakage is often ignored in other analytical methods, but is shown to affect long-term storage sizing, and can cause energy deficits in the system.
- Two solar–battery case studies demonstrate the method. The first case study shows the optimal size does not have wasted capacity due to over-sizing, nor cause energy deficits due to under-sizing. The second case study shows increasing storage size has a diminishing return on storage energy provided, and relates the diminishing return thresholds to the largest daily and annual storage designs.

The paper is structured as follows. Section 2 introduces the storage sizing method. Section 3 presents the benchmark and two case studies on sizing storage with surplus generation and excess demand. Section 4 concludes the paper.

2. Method

The proposed algorithm sizes storage based on the largest cumulative charge or discharge the storage can experience. The paper first establishes the equation for constructing storage profiles. The difference between critical points in the storage profile determines the cumulative charge or discharge. The paper proposes a matrix to calculate these differences. Based on the storage profile trend, the largest cumulative charge or discharge is extracted from the matrix, yielding the storage size. An iterative method is then added to account for the storage's

energy limits, power limits, and energy leakage. Finally, the sizing algorithm is combined with the Monte Carlo simulation to account for uncertainties in generation and demand. The paper aims to demonstrate the sizing method using a microgrid setup, a conventional operation control strategy, and a simple storage model.

2.1. Storage profile

The independent microgrid has three main components: renewable generation, electricity demand, and energy storage, as shown in Fig. 1. The system uses a conventional operation control strategy to maximize renewable consumption, where renewable generation is the primary energy supply, and storage is the secondary supply [13]. The precedence means renewable generation is used first to meet the demand. Once the demand is satisfied, excess generations are charged into energy storage. However, when generation alone cannot meet the demand, storage discharges energy to meet the demand. When storage does not have enough energy to discharge, the demand cannot be met, and an energy deficit occurs.

Fig. 1(a) shows the scenario when generation is greater than demand. Part of the generation ($G(t)$) directly supplies the demand ($D(t)$), while the remaining surplus generation ($G(t) - D(t)$) is charged into storage. The storage energy's ($S(t)$) rate of change due to charging is the product of surplus generation and charge efficiency (η_c). Fig. 1(b) shows the scenario when generation cannot meet the demand. Generation directly supplies the demand, and the remaining unmet demand ($D(t) - G(t)$) is supplemented by storage. The product of the storage energy's rate of change due to discharging and the discharge efficiency (η_d), is equal to the power required to supplement the unmet demand. Rearranging the equation shows the change in storage energy is equal to the negative of unmet demand divided by the discharge efficiency. The storage behaviors from both scenarios in Fig. 1 are modeled by Eq. (1).

$$\frac{dS(t)}{dt} = (G(t) - D(t))\eta_c, \quad (1)$$

$$\text{where: } \eta(t) = \begin{cases} \eta_c, & \text{if } G(t) - D(t) > 0, \\ \frac{1}{\eta_d}, & \text{if } G(t) - D(t) < 0. \end{cases}$$

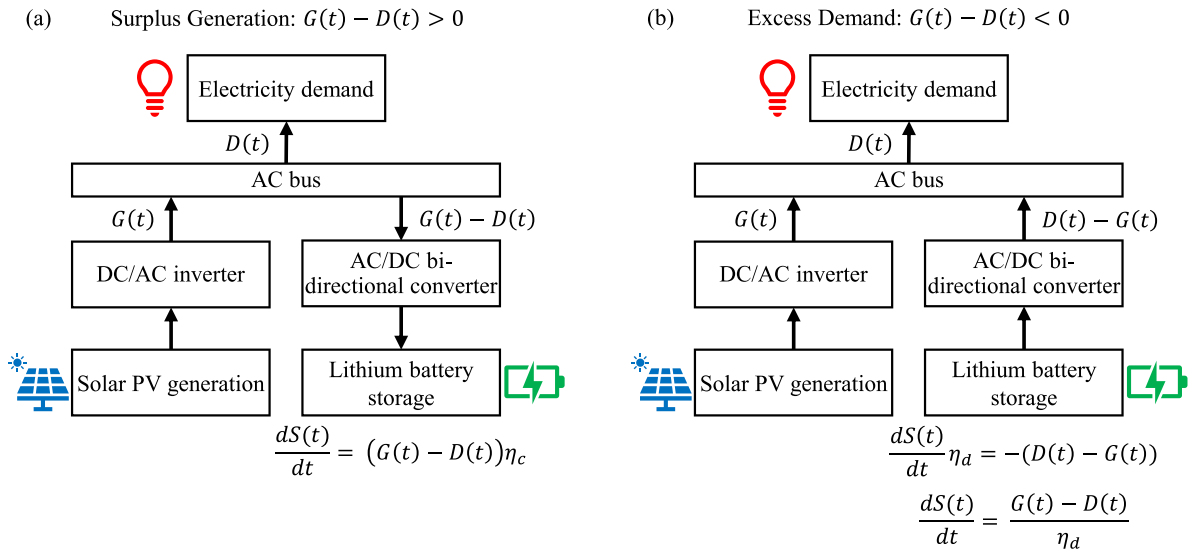


Fig. 1. Independent microgrid setup and control in scenarios with (a) surplus generation and (b) excess demand. The microgrid is controlled using a conventional operation strategy to maximize renewable consumption. The equations model the change in lithium battery's stored energy (S) in relation to generation (G), demand (D), and storage efficiency (η). The arrows indicate power flow directions.

Eq. (1) is integrated from the current time step (t) to a future time step ($t + \Delta t$) to calculate the change in storage level. The integration is calculated via linear approximation by assuming the time interval is small, such that dt is approximated using Δt . The approximation means demand, generation, and storage efficiency are constant during each small time interval. The integration yields Eq. (2), which is time-discrete.

$$\begin{aligned} \int_t^{t+\Delta t} \frac{dS(t)}{dt} dt &= \int_t^{t+\Delta t} (G(t) - D(t)) \eta(t) dt, \\ S(t + \Delta t) - S(t) &= (G(t) - D(t)) \eta(t) \Delta t, \\ S(t + \Delta t) &= S(t) + (G(t) - D(t)) \eta(t) \Delta t, \end{aligned} \quad (2)$$

where: $\eta(t) = \begin{cases} \eta_c, & \text{if } G(t) - D(t) > 0, \\ \frac{1}{\eta_d}, & \text{if } G(t) - D(t) < 0, \end{cases}$

The equation says the storage energy level at a future time step ($S(t + \Delta t)$) is equal to the current storage level ($S(t)$) plus the change in storage level. The change in storage level is equal to the difference between generation ($G(t)$) and demand ($D(t)$), multiplied by the storage efficiency ($\eta(t)$) and time interval (Δt).

For short-term storage sizing, Eq. (2) is sufficient. Note the time frame for short-term storage depends on the storage device. For example, a lithium battery loses 2% of its energy per month due to self-discharge [46], while a flywheel energy storage can lose more than 20% of its kinetic energy per hour due to friction [47]. Eq. (2) is modified to account for energy loss from storage leakage, forming Eq. (3).

$$\begin{aligned} S(t + \Delta t) &= S(t)(1 - \sigma) + (G(t) - D(t)) \eta(t) \Delta t, \end{aligned} \quad (3)$$

where: $\eta(t) = \begin{cases} \eta_c, & \text{if } G(t) - D(t) > 0, \\ \frac{1}{\eta_d}, & \text{if } G(t) - D(t) < 0, \end{cases}$

$\sigma = 0$, if $S(t) < 0$,

Where σ is the storage energy leakage rate. The equation is used to construct the storage profile. During construction, the leakage rate is zero if the storage level falls below zero. The model can be applied to most energy storage devices controlled using a conventional operation strategy.

2.2. Storage sizing

The method sizes storage based on the largest increase or decrease in the storage profile, equivalent to the largest cumulative charge or discharge the storage can experience over the design period. The increases and decreases are calculated via the difference between critical points in the storage profile. Eq. (4) calculates the critical points by setting the storage profile's derivative equal to zero and finding the roots.

$$\text{Solve } \frac{dS(t)}{dt} = 0 \text{ for all } t, \quad (4)$$

such that critical points are: t_1, t_2, \dots, t_n ,

and critical storage levels are: $S(t_1), S(t_2), \dots, S(t_n)$.

Moreover, computer functions, such as "argrextrema" in SciPy, find critical points by comparing each point with their preceding and following points [48]. If a point's storage level is higher or lower than the neighboring point's storage levels, then it is a critical point. In rare cases, if both the starting and ending storage levels are higher or lower than their neighboring storage levels, then they are also critical points.

The critical points' storage levels are used by the difference matrix \mathbf{D} in Eq. (5) to calculate the storage level differences required for storage sizing. The Appendix contains the proof that shows the difference matrix captures all storage level differences required for storage sizing.

$$\mathbf{D} = \mathbf{L} + \mathbf{C} - \mathbf{C}^T, \quad (5)$$

$$\begin{aligned} \text{where : } \mathbf{L} &= \begin{cases} l_{(i,j)} = 0, & \text{if } i \leq j, \\ l_{(i,j)} = S(T) - S(0), & \text{if } i > j, \end{cases} \\ \mathbf{C} &= \mathbf{1}_n^T \mathbf{C}_n, \\ \mathbf{1}_n &= [1, 1, \dots, 1], \\ \mathbf{C}_n &= [S(t_1), S(t_2), \dots, S(t_n)], \end{aligned}$$

The resulting matrix \mathbf{D} :

$$\begin{bmatrix} 0 & S(t_2) - S(t_1) & \dots & S(t_n) - S(t_1) \\ (S(T) - S(0)) + S(t_1) - S(t_2) & 0 & \dots & S(t_n) - S(t_2) \\ \vdots & \vdots & \ddots & \vdots \\ (S(T) - S(0)) + S(t_1) - S(t_n) & (S(T) - S(0)) + S(t_2) - S(t_n) & \dots & 0 \end{bmatrix}$$

In essence, matrix \mathbf{D} pairs critical storage levels and calculates the difference between them. $\mathbf{L} + \mathbf{C}$ produce the first half of the pairs, and \mathbf{C}^T produce the second half. Matrix \mathbf{C} is created via the dot product of the transposed horizontal vector of all-ones ($\mathbf{1}_n^T$) and the horizontal vector of critical storage level (\mathbf{C}_n). Matrix \mathbf{L} is a lower triangular matrix, where the lower-left half below the diagonal is filled with the difference value between the starting ($S(0)$) and ending storage levels ($S(T)$). The purpose of matrix \mathbf{L} is to push the lower-left half of matrix \mathbf{C} into the second design period, as storage levels in the second period can also govern the sizing. The maximum and minimum of matrix \mathbf{D} correspond to the largest increase and decrease in the storage profile.

Eq. (6) states that storage size depends on the difference matrix \mathbf{D} and the overall storage profile trend.

$$E = \begin{cases} |\text{Min}(\mathbf{D})|, & \text{if } S(T) - S(0) > 0, \\ \text{Max}(\mathbf{D}), & \text{if } S(T) - S(0) < 0, \\ \text{Max}|\mathbf{D}|, & \text{if } S(T) - S(0) = 0, \end{cases} \quad (6)$$

If the overall storage profile increases, that is, the ending storage level ($S(T)$) is greater than the starting storage level ($S(0)$), then storage size (E) is equal to the absolute value of the difference matrix's minimum ($|\text{Min}(\mathbf{D})|$), corresponding to the largest decrease in the storage profile. Conversely, if the overall storage profile decreases ($S(T) - S(0) < 0$), then storage size is equal to the difference matrix's maximum ($\text{Max}(\mathbf{D})$), corresponding to the storage profile's largest increase. Lastly, if the overall storage profile neither increases nor decreases ($S(T) - S(0) = 0$), then storage size is equal to the maximum absolute value of the difference matrix ($\text{Max}|\mathbf{D}|$), corresponding to the storage profile's largest absolute increase or decrease. The following three paragraphs explain the theories behind the equation's three scenarios.

When the overall storage profile increases, more energy has been charged into storage than discharged, due to an overall surplus of generation. The surplus indicates total generation is more than enough to support the system. In this scenario, the storage's purpose is to store just enough energy to supplement periods where generation cannot support the system. During these periods, the storage discharges energy, corresponding to decreases in the storage profile. If storage is sized to accommodate the largest cumulative discharge, it can also accommodate any smaller discharges. Thus, when the overall storage profile increases, storage is sized to accommodate the largest cumulative discharge, corresponding to the largest decrease in the storage profile.

When the overall storage profile decreases, storage has discharged more energy than charged due to an overall excess of demand. The excess demand indicates that the total generation is insufficient to support the system. In this scenario, the storage's purpose is to meet as much demand as possible, by storing as much energy as possible. To do this, storage needs to charge as much energy as possible during surplus generations, corresponding to increases in the storage profile. If the storage is sized to accommodate the largest cumulative charge, it can also accommodate any smaller charges, enabling the storage to store as much energy as possible. Thus, when the overall storage profile decreases, storage is sized to accommodate the largest cumulative charge, corresponding to the largest increase in the storage profile.

When the overall storage profile neither increases nor decreases, storage has discharged as much energy as charged, indicating that the total generation is just enough to support the system. In this scenario, the storage's purpose is to charge from surplus generations and discharge to meet the excess demands. Suppose the storage is sized to accommodate the largest cumulative charge or discharge. In that case, storage can also accommodate any smaller charges and discharges, enabling it to store surplus generations to meet the excess demands. Thus, when the overall storage profile neither increases nor decreases, storage is sized to accommodate the largest cumulative charge or discharge, corresponding to the largest absolute increase or decrease in the storage profile.

In essence, when storage has charged more energy than discharged, size for the limiting factor that is the largest cumulative discharge. Vice versa, when storage has discharged more than charged, size for the largest cumulative charge.

2.3. Storage lifespan

Battery manufacturers specify cycle life under specific depth of discharge and C-rating to preserve battery health and ensure the intended lifespan of the battery. For example, lithium batteries can have a cycle life of 2,000 cycles, under the conditions the maximum depth of discharge is 80% of the original battery capacity, and the C-rating is 1C. The maximum depth of discharge limits deep discharge, while C-rating limits high charge and discharge rates; both of which can damage battery health and shorten cycle life [49]. Cycle life is the number of cycles the battery can charge and discharge before the storage capacity degrades to 80% of the original capacity. Thus, limiting the depth of discharge ensures the battery has enough capacity over its cycle life while accounting for degradation, and the battery should be replaced at the end of cycle life. Eq. (7) calculates the storage's total energy capacity when accounting for the depth of discharge.

$$E_{tot} = \frac{E}{DoD_{max} - DoD_{min}}, \quad (7)$$

The equation says storage's total energy capacity (E_{tot}) is equal to the storage size (E) divided by the difference between the maximum (DoD_{max}) and minimum depth of discharge (DoD_{min}). In this design method, storage size is the energy capacity in the usable portion of the storage, while the remaining capacity is reserved to compensate for storage degradation.

Storage cannot discharge beyond the maximum depth of discharge, nor charge above the minimum depth of discharge. The storage levels at the maximum and minimum depth of discharge define the storage's energy limits. The upper and lower storage energy limits are defined by Eqs. (8) and (9), respectively.

$$S_{up} = E_{tot} (1 - DoD_{min}), \quad (8)$$

$$S_{low} = E_{tot} (1 - DoD_{max}), \quad (9)$$

Where S_{up} and S_{low} are the upper and lower storage limits, E_{tot} is storage's total energy capacity, DoD_{max} and DoD_{min} are the maximum and minimum depth of discharge.

The storage's energy limits are used in Eq. (10) when constructing the constrained storage profile.

$$S_{low} \leq S(t) \leq S_{up}, \quad (10)$$

The equation says the storage level ($S(t)$) cannot exceed the upper storage limit (S_{up}), nor fall below the lower storage limit (S_{low}). Once the storage level hits the upper limit, energy cannot be charged into storage. Vice versa, energy cannot be discharged if the storage level is at the lower limit, preventing deep discharge that can damage battery cycle life.

Eq. (10) should hold in the final constrained storage profile. However, it is often too restrictive when used in the iterative storage

sizing method, which can cause near-optimal sizing. To solve this issue, Eq. (11) relaxes the energy limit constraint by adding a slack term, allowing the storage level to go beyond the storage energy limits.

$$S_{low} - \alpha |S(T) - S(0)| \leq S(t) \leq S_{up} + \alpha |S(T) - S(0)|, \quad (11)$$

where: $0 \leq \alpha < 1$,

The slack is the absolute difference between the last iteration's starting ($S(0)$) and ending storage levels ($S(T)$), scaled by a multiplier (α). The multiplier is a number between zero and one. A large multiplier will cause slow convergence or even non-convergence, while a small multiplier may yield near-optimal sizing instead of the exact optimal. A multiplier of 0.5 will work for most cases. However, a better strategy is to start with a large multiplier, then gradually reduce it at each iteration. The constraint pushes the storage profile into a sustainable state, while the slack term ensures it does not push too hard to cause near-optimal sizing.

A constrained storage profile will repeat itself when subject to the same demand and generation patterns in the future. The repeatability ensures the storage size is sustainable, and can support similar demand and generation patterns in the future. Equal starting and ending storage levels characterize sustainability. The sustainable starting storage level is calculated using Eq. (12).

$$S(0)_s = \begin{cases} S(T) - \text{Max}(S(t)) + S_{up}, & \text{if } S(T) - S(0) \geq 0, \\ S(T) - \text{Min}(S(t)) + S_{low}, & \text{if } S(T) - S(0) \leq 0, \end{cases} \quad (12)$$

Where $S(0)_s$ is the sustainable starting storage levels, $S(0)$ and $S(T)$ are the starting and ending storage levels in the storage profile, $\text{Max}(S(t))$ and $\text{Min}(S(t))$ are the maximum and minimum storage levels in the storage profile, S_{up} and S_{low} are the upper and lower storage limits. The equation says the sustainable starting storage level is dictated by the difference between the ending and maximum storage levels in an increasing scenario, and by the ending and minimum storage levels in a decreasing scenario. The storage limits are added to re-frame those differences to the usable portion of storage.

High charge and discharge rates can also damage battery health and shorten cycle life [50]. The C-rating relates the battery's energy capacity to power capacity. The maximum charge and discharge rate are calculated based on the C-ratings using Eqs. (13) and (14), which define the storage's power limits.

$$P_c = E_{tot} C_c, \quad (13)$$

$$P_d = E_{tot} C_d, \quad (14)$$

Where P_c and P_d are the maximum charge and discharge rates, E_{tot} is the storage's total energy capacity, C_c and C_d are the storage's charge and discharge C-ratings. Moreover, the external power structure connected to the storage can also limit charge and discharge rates.

The power limits are used in Eq. (15) while constructing the constrained storage profile.

$$-P_d \leq G(t) - D(t) \leq P_c, \quad (15)$$

The equation says power charged to or discharged by storage ($G(t) - D(t)$) cannot exceed the maximum charge (P_c) or discharge rates (P_d). The equation limits high charge and discharge rates that can damage battery health.

Eq. (15) should hold in the final constrained storage profile; however, it is often too restrictive when used in the iterative storage sizing method. In particular, if storage size becomes zero during an iteration, the power limits will also become zero, causing storage size in all subsequent iterations to be zero. Eq. (16) relaxes the power limit constraint by adding a slack term, enabling zero storage size to have charge and discharge.

$$-P_d - \alpha |S(T) - S(0)| \leq G(t) - D(t) \leq P_c + \alpha |S(T) - S(0)|, \quad (16)$$

where: $0 \leq \alpha < 1$,

The slack is the absolute difference between the last iteration's starting ($S(0)$) and ending storage levels ($S(T)$), scaled by a multiplier (α).

The storage lifespan is calculated using Eq. (17).

$$T_{life} = \text{Min}(T_{cal}, \phi \frac{NE}{Q}) \quad (17)$$

Where T_{life} is the battery lifespan in years, T_{cal} is the battery calendar life, ϕ is the degradation factor, N is the battery cycle life, E is the storage size, and Q is the battery energy throughput over a year. The energy throughput is calculated by summing either the charge or discharge energy in the final constrained storage profile. The manufacturer specifies the battery cycle life and calendar life in terms of number of cycles and number of years, respectively. The degradation factor is a number less than one, which depends on the application of the battery. For example, the degradation factor is smaller with solar-battery systems, as solar intermittency can cause rapid charge and discharge from the battery, damaging the battery and shortening its lifespan.

2.4. Iterative storage sizing

The sizing method is extended iteratively to account for the depth of discharge, maximum charge and discharge rates, and energy leakage. These elements have inter-dependency with the storage size, therefore requiring an iterative approach to solve. The sizing steps are outlined in Fig. 2.

The first step is to construct the unconstrained storage profile using Eq. (2). Then, identify critical points in the storage profile using Eq. (4)

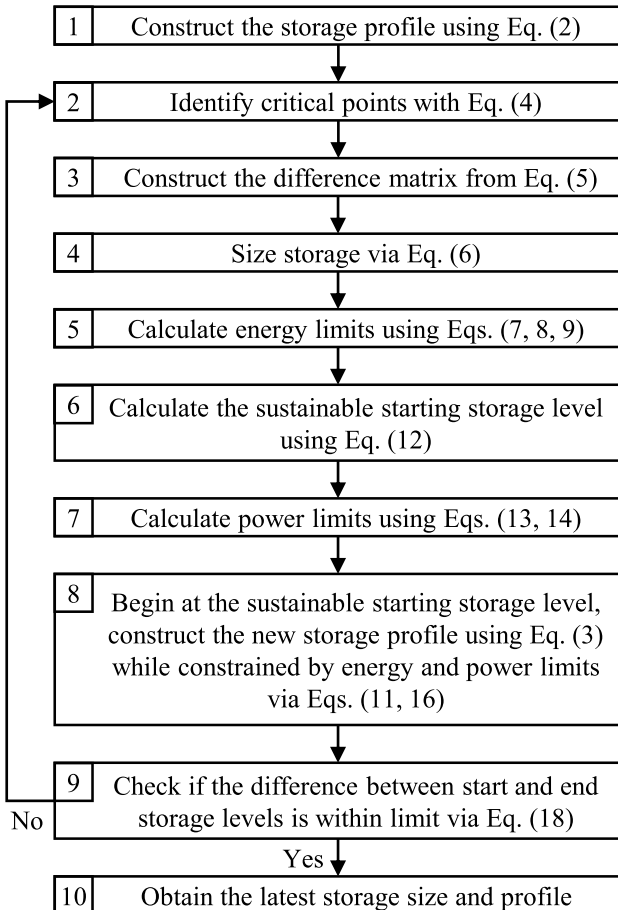


Fig. 2. The storage sizing steps flowchart. The sizing method uses the equations to calculate the optimal storage size and associated constrained storage profile.

or computer functions. The critical points' storage levels are used in Eq. (5) to construct the difference matrix, and the storage size is calculated using the difference matrix via Eq. (6). The storage size is used in Eqs. (7), (8), and (9) to calculate the upper and lower storage limits. The storage limits are then used in Eq. (12) to calculate the sustainable starting storage level. Then, the maximum charge and discharge rates are calculated using Eqs. (13) and (14). The eighth step is to construct the new storage profile. Starting from the sustainable starting storage level, the new profile is constructed using Eq. (3), while constrained by the relaxed storage energy limits via Eq. (11), and by the relaxed storage power limits via Eq. (16). The new constrained storage profile is used in the ninth step, to check if the absolute difference between starting and ending storage levels is within the user-defined permissible limit, as stated in Eq. (18).

$$|S(T) - S(0)| \leq \epsilon, \quad (18)$$

The permissible difference limit (ϵ) dictates the accuracy and significant figures of the resulting storage size. If the difference is beyond the limit, then repeat the process from the second step with the new constrained storage profile. If the difference is within the limit, then the latest storage size and constrained storage profile are the results.

2.5. Monte Carlo simulation

Monte Carlo simulation accounts for the uncertainties in renewable generation and electricity demand. The simulation first generates randomized generation and demand profiles using statistical models. The randomized profiles are fed into the storage sizing algorithm to obtain a distribution of optimal storage sizes. The optimal storage size is then selected based on the distribution. The steps for the Monte Carlo simulation are outlined in Fig. 3.

The first step is to calculate the mean and standard deviation of the historical data at each time step. The mean and standard deviation are calculated using Eqs. (19) and (20), respectively.

$$\bar{x} = \frac{1}{n} \sum_{i=1}^n x_i \quad (19)$$

$$s = \sqrt{\frac{1}{n-1} \sum_{i=1}^n (x_i - \bar{x})^2} \quad (20)$$

Where at a particular time step, x is the historical data, n is the number of historical data, \bar{x} is the mean or average value, and s is the standard

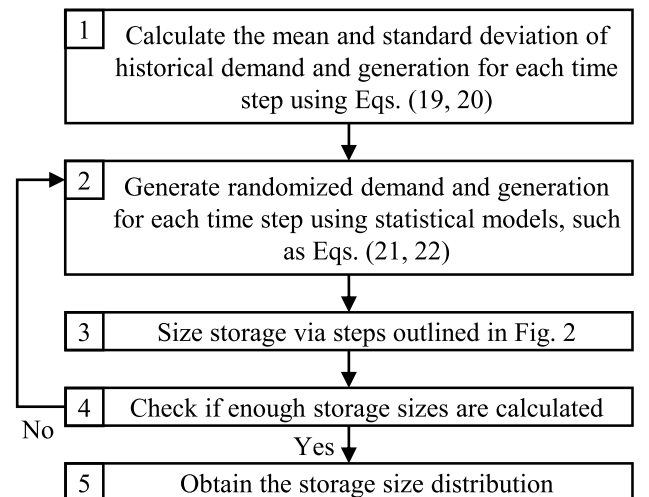


Fig. 3. Monte Carlo simulation steps flowchart. The simulation enables the sizing algorithm to size storage while accounting for generation and demand uncertainties.

deviation. For example, historical data from the first hour of the year, for the past ten years, are used to calculate the mean and standard deviation for the first time step.

The second step is to generate randomized demand and generation profiles using probability distribution models. In this study, variations in demand and generation at each time step are assumed to follow the normal distribution [20]. Randomized data following normal distribution are generated using Box–Muller transform via Eqs. (21) and (22).

$$r_{n1} = \sqrt{-2 \ln r_{u1}} \cos(2\pi r_{u2})s + \bar{x} \quad (21)$$

$$r_{n1} = \sqrt{-2 \ln r_{u1}} \sin(2\pi r_{u2})s + \bar{x} \quad (22)$$

Where r_{n1} and r_{n2} are two randomized data following the normal distribution with specified mean (\bar{x}) and standard deviation (s). r_{u1} and r_{u2} are two random values between zero and one, generated via uniform distribution. The Box–Muller transform takes two random values between zero and one, and generates two randomized values following the normal distribution. Other statistical models can also model the uncertainties in generation and demand, such as Weibull and Gamma distributions.

The third step is to feed the randomized demand and generation profiles into the storage sizing algorithm outlined in Fig. 2, and calculate the storage size. Then, repeat this process from the second step until enough storage sizes are calculated. Finally, gather the results to form a distribution of storage sizes. The distribution gives useful information, such as the mean and standard deviation. The percentile of each storage size can also be calculated by ranking the storage sizes from small to large.

3. Case studies and results

This section benchmarks the proposed method and presents two case studies. The proposed method is benchmarked against mathematical, meta-heuristic, and enumerative optimizations. The two case studies present scenarios with overall surplus generation and excess demand. The first case study demonstrates the sizing method, and shows the optimal size does not have wasted storage due to over-sizing, nor cause energy deficits due to under-sizing. The study also shows energy leakage can affect long-term storage sizing. The second case study shows storage size requirements are high during early summer and early autumn, when both generation and demand are high. The study also shows increasing storage size has diminishing returns on

storage energy provided, and relates the diminishing return thresholds to the largest daily and annual storage designs.

3.1. Benchmark

The proposed method was tested on randomly generated scenarios against other sizing methods, including: the one-by-one enumerative method for benchmarking, particle swarm meta-heuristic algorithm for locating global optimal, and Gurobi mathematical programming for speed comparison. The comparison between the methods is shown in Table 1. The proposed method is faster than other methods, calculates the exact optimal, handles non-linear models, and is built on a real-world theory. The fast speed is helpful in applications with repeated sizing, such as the Monte Carlo method. The ability to calculate exact optimal yields more precise and accurate answers. The capability to handle non-linear models enables more detailed and accurate storage modeling. Finally, the proposed optimization algorithm is based on a real-world theory that states storage should be sized according to the largest cumulative charge or discharge it can experience. This real-world connection enables a deeper understanding of the sizing method.

Three limitations of the proposed method were identified during testing. The first limitation is that while the proposed method is initially faster, other methods can eventually catch up. The proposed method's calculation time is related to the number of critical points in the storage profile. In contrast, other methods' calculation times are related to the total number of data points in the profile. Since the number of critical points is a fraction of all data points, the proposed method is initially faster. However, the proposed method has a time complexity of $O(n^2)$ due to the matrix used, while other methods have a time complexity of $O(n)$. The time complexity indicates that other methods' calculation times are linearly related to the number of data points. In contrast, the proposed method's calculation time is quadratically related to the number of critical points. Thus, while the proposed method is initially faster, other methods can eventually catch up as the data size increases. Each method's calculation speed trendline is shown in Fig. 4. The speed tests are done using an Intel Core i7-9700 processor with randomly generated data. The data size increased at 1,000 data points increments, and tests were repeated 30 times at each increment.

The second limitation is that the proposed method yields the largest storage size without wasted storage. In some scenarios, this storage size does not provide the maximum amount of energy to the system, as storage wastage is needed to maximize the energy provided. These scenarios usually have a high leakage rate of more than 40% per

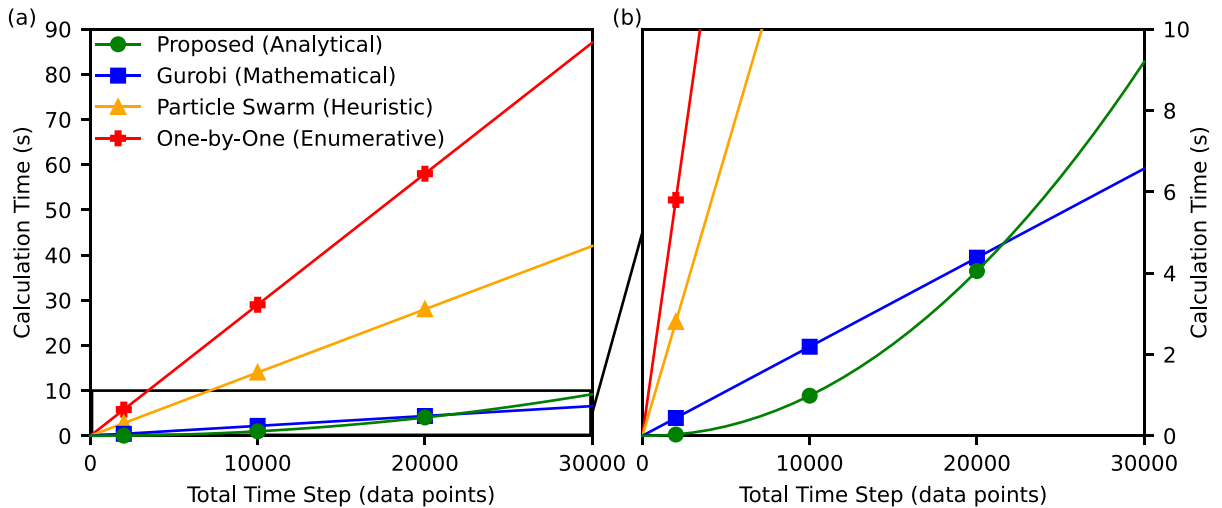


Fig. 4. Storage sizing methods' speed comparison via (a) calculation time trendlines and (b) zoomed-in window of the trendlines. In the zoomed-in window, the Gurobi mathematical programming method becomes faster than the proposed method at 22,000 data points.

time interval, and small charge and discharge rates of less than 0.1C relative to the storage capacity. In these scenarios, the storage will have a larger energy capacity to increase the charge and discharge rates. However, the larger energy capacity is not fully utilized, as storage will operate at low storage levels to reduce energy leakage. Thus, the storage size providing maximum energy will have wasted capacity in these scenarios, and the method will yield the closest storage size without wasted capacity.

The third limitation is that the current battery lifespan model is simple, but can be inaccurate. The current model uses lithium battery manufacturer's recommended depth of discharge and C-rating to preserve battery health, and achieve the specified cycle life. However, studies have shown that renewable intermittency can stress the battery and shorten its lifespan [39]. Lithium battery degradation modeling is an active research area, and many models have been proposed in recent years [51]. Factors such as usage, time, temperature, depth of discharge, charge and discharge rates, voltage, and state of charge can all contribute to lithium battery degradation [49].

3.2. Size storage with surplus generation

A hypothetical solar photovoltaic (PV) and lithium battery microgrid system is used to demonstrate the storage sizing method. The

microgrid setup is shown in Fig. 1, and the system is controlled using a conventional operation strategy to maximize renewable consumption [13]. The operation strategy will first use solar generation to meet the demand directly. Once the demand is met, any excess generation is charged into storage. When generation cannot meet the demand, energy is discharged from storage to meet the demand. When storage does not have enough energy to discharge, the demand cannot be met, and an energy deficit occurs. The solar PV system has an annual generation of 7.2 MWh, and the microgrid's annual electricity demand is 6 MWh. The microgrid system is situated in a northern temperate climate, with warm summers and cold winters. The monthly total generation and demand profiles are shown in Fig. 5. The generation profile follows the typical solar generation pattern in the northern temperate zone, with high generations during summer and low during winter. Similarly, the demand profile follows the typical electricity demand pattern in the northern temperate zone, with high summer demands and low winter demands.

The lithium battery storage system is assumed to have a charge and a discharge efficiency of 0.8 [40]. The storage level starts at zero, and storage levels at the end of each month are calculated using Eq. (2). The resulting unconstrained storage profile is shown in Fig. 5. The profile starts in the winter and initially decreases as storage discharges

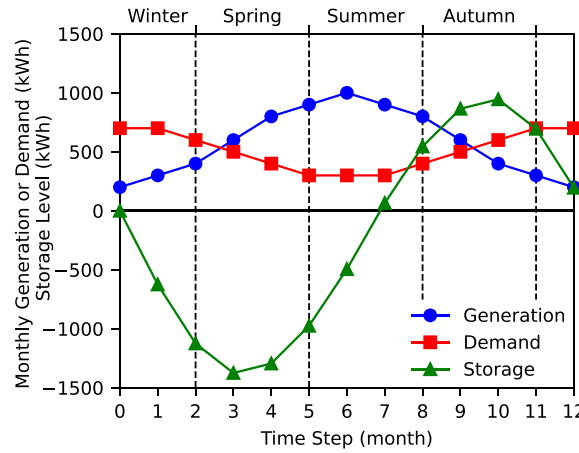


Fig. 5. Solar-battery microgrid's monthly total solar PV generation, electricity demand, and the lithium battery's unconstrained storage profile. The microgrid is controlled to maximize renewable consumption. In the generation and demand profiles, the nodes represent monthly total energy, and the month begins at the node. In the storage profile, the nodes represent lithium battery's stored energy at each time step. The dashed lines separate the seasons.

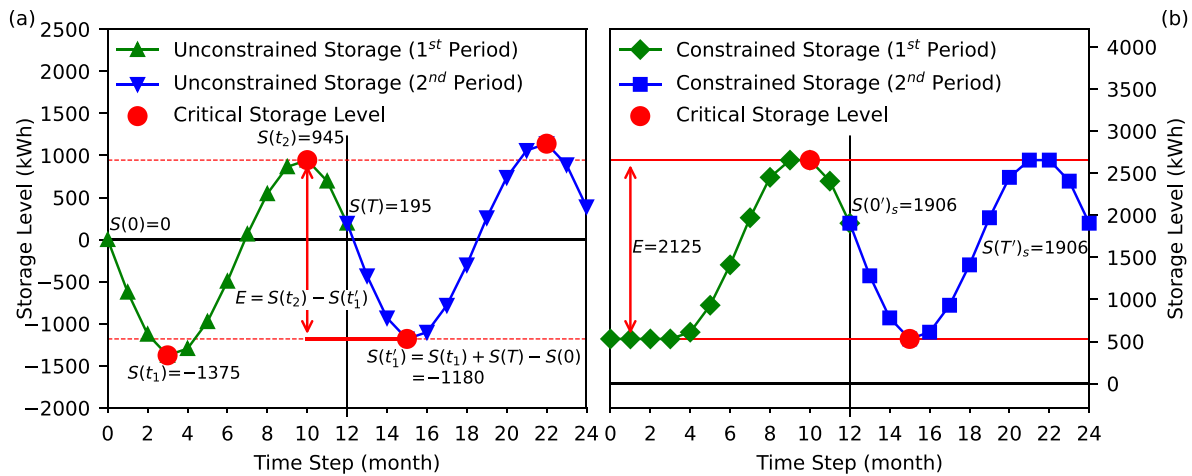


Fig. 6. Solar-battery microgrid's (a) unconstrained storage profile and (b) constrained storage profile. The unconstrained storage profile shows the critical storage levels used to calculate the storage size (E). The storage size is used to construct the constrained storage profile. In the constrained profile, the red horizontal lines mark the upper and lower storage limits according to 80% depth of discharge. Storage cannot charge beyond the upper limit nor discharge below the lower limit. (For interpretation of the references to color in this figure legend, the reader is referred to the web version of this article.)

energy to supplement the high winter demand. The decrease stops in early spring, as the rising solar generation balances the falling demand, allowing the generation to satisfy demand directly. Then the profile increases during late spring, summer, and early autumn, as storage charges from the surplus solar generation. The increase stops in late autumn, as the rising demand balances with the falling generation. Finally, the profile decreases again during late autumn and winter due to the excess demand. Overall, the storage profile increased between the start and end of the year, indicating more generation than demand across the year.

Fig. 6(a) shows the unconstrained storage profile extended to two design periods (years) with critical points identified. In the first period, the ending storage level ($S(T)$) is greater than the starting storage level ($S(0)$), meaning the overall storage profile increases. In an increasing scenario, storage is sized according to the profile's largest decrease, corresponding to the largest cumulative discharge the storage can experience. The largest decrease starts from the second critical storage level in the first period ($S(t_2)$), and ends at the first critical storage level in the second period ($S(t'_1)$). Correspondingly, the largest cumulative discharge starts in late autumn and ends in early spring, during which excess demands cause the storage to discharge. To size the storage, the difference matrix is constructed using Eq. (5). Then, Eq. (6) says in an increasing scenario, storage size is equal to the absolute value of the difference matrix's minimum, which is 2125 MWh.

Lithium batteries have a recommended depth of discharge of 80% [52], and using Eq. (7), the total storage capacity is calculated to be 2656 kWh. The upper and lower storage limits are calculated using Eqs. (8) and (9) to be 2656 kWh and 531 kWh, respectively. Moreover, lithium batteries typically have charge and discharge C-ratings of 1C [53], which means the maximum charge and discharge rates are 2656 kW according to Eqs. (13) and (14). The constrained storage profile is constructed using Eq. (2) while constrained by the storage energy limits via Eq. (10) and by the power limits via Eq. (15).

Fig. 6(b) shows the constrained storage profile. The profile starts during winter, where it stays at the lower storage limit due to excess winter demands. In early spring, the demand falls while solar generation rises, creating surplus generations to charge the storage, causing the profile to increase. During summer, the profile continues to increase as storage continues to charge. The upper storage limit is reached in early autumn. The storage is sized to store just enough energy to carry through the largest cumulative discharge during late autumn, winter, and early spring. In late autumn, storage begins to discharge due to excess demands, causing the profile to decrease. The storage continues to discharge during winter, and the profile briefly reaches the lower storage limit in early spring. Then, mid-spring begins, and the profile starts to increase as storage charges from the surplus generation again.

In the second period (year) of the constrained storage profile in Fig. 6(b), the ending storage level is the same as the starting storage level. The equal starting and ending storage levels show that the constrained storage profile is sustainable, and can repeat itself indefinitely if generation and demand patterns do not vary significantly from year to year. The repeatability ensures that the storage size is not only valid for the current design period, but also for future periods. The sustainable starting storage level is calculated to be 1906 kWh using Eq. (12).

Fig. 7 shows the constrained storage profiles for optimally sized, oversized, and undersized storage during three periods (years). For the undersized storage shown in Fig. 7(c), the storage profile starts empty at the lower storage limit during winter. It begins to increase in mid-spring, and reaches the undersized capacity in summer. Then, the profile starts to decrease in late autumn. Due to the undersizing, the storage does not have enough stored energy to carry through the largest cumulative discharge between late autumn and early spring. As a result, the storage empties in winter, and stays empty until mid-spring. The empty storage cannot provide energy to meet the demands,

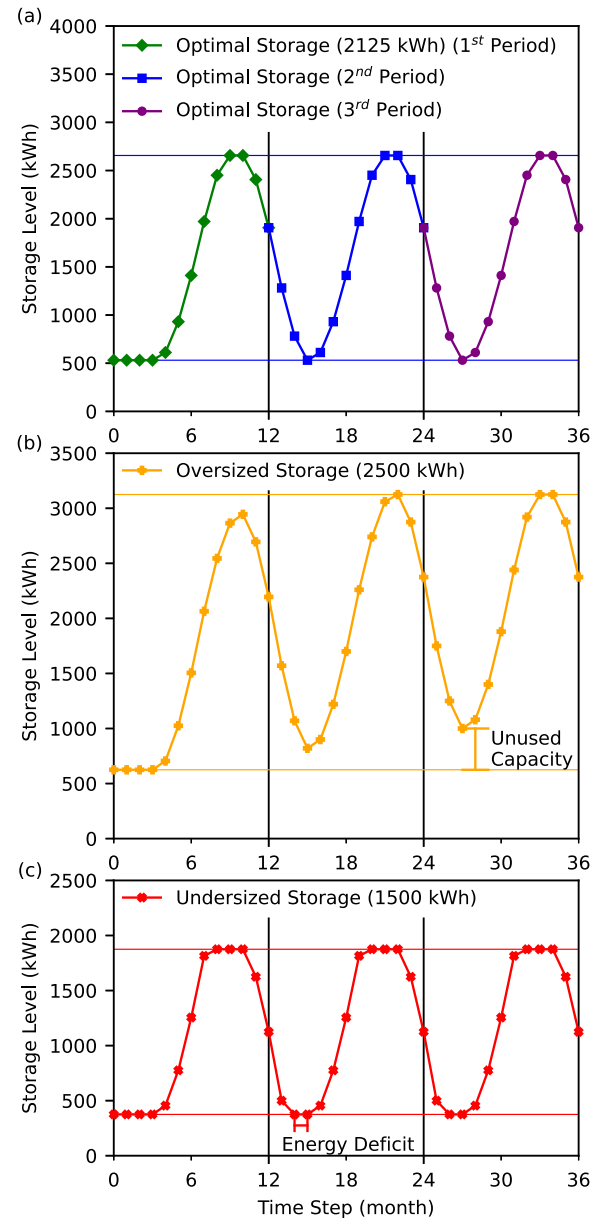


Fig. 7. Constrained storage profile of (a) optimally sized, (b) oversized, and (c) undersized storage. The profiles encompass three design periods (years). The colored horizontal lines mark the upper and lower storage limits according to 80% depth of discharge. Storage cannot charge beyond the upper limit nor discharge below the lower limit, and energy deficits occur when storage cannot discharge to meet the demand. The figure shows optimally sized storage does not have wasted capacity due to over-sizing, nor cause energy deficits due to under-sizing. (For interpretation of the references to color in this figure legend, the reader is referred to the web version of this article.)

causing energy deficits. In contrast, the oversized storage shown in Fig. 7(b) never reaches empty, as it has more than enough capacity to carry through the largest cumulative discharge. However, part of the capacity is wasted and never used. Compared to oversized and undersized storage, the optimally sized storage shown in Fig. 7(a) does not have wasted storage capacity due to over-sizing, nor cause energy deficits due to under-sizing. Thus, the optimal size is the largest storage size that provides the maximum amount of energy to the system without wasted capacity. Note that one may still choose a larger storage for the greater safety factor, or a smaller storage for the cheaper cost.

The design period is a year, which is considered long-term for lithium batteries. When sizing for long-term storage, energy leakage

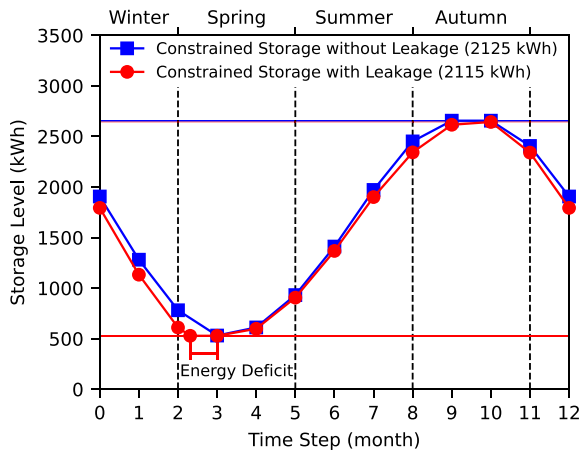


Fig. 8. Constrained storage profiles with and without accounting for energy leakage. The colored horizontal lines mark the upper and lower storage limits. Storage cannot charge beyond the upper limit nor discharge below the lower limit, and energy deficits occur when storage cannot discharge to meet the demand. The dashed lines separate the seasons. (For interpretation of the references to color in this figure legend, the reader is referred to the web version of this article.)

can have significant impacts. Lithium batteries are assumed to have a constant energy leakage rate of 2% per month [46]. The iterative sizing method is used to account for leakage. Beginning at the sustainable starting storage level, the storage profile with leakage is constructed via Eq. (3) while constrained by Eqs. (11) and (16). Following the steps outlined in Fig. 2, the iterative sizing method is conducted using a multiplier of 0.1 and a permissible difference limit of 0.01. The storage size converged at 2115 kWh after seven iterations. Compared to the original sizing, the storage size decreased because leakage reduced the amount of energy in the storage. Fig. 8 shows the constrained storage profiles with and without leakage. When compared, the profile with leakage decreases faster and increases slower, indicating the storage effectively discharges faster and charges slower due to leakage. The profile with leakage also shows that storage size is insufficient to carry through the largest cumulative discharge, and energy deficits will occur in early spring. The energy deficit indicates generation can no longer fully support the demand with the additional loss from storage leakage. Therefore, it is crucial to account for storage leakage when sizing for long-term energy storage.

3.3. Size storage with excess demand

The storage sizing method is applied to a domestic property in Oxfordshire. The owner plans to install roof-top solar PV panels and wants to know what size of lithium battery storage can complement the solar PV. The solar-battery system setup is shown in Fig. 9. The microgrid system consists of a common AC bus that connects all the elements. The grid electricity network connects to the bus, and regulates the microgrid's frequency and voltage. The electricity demand directly taps from the bus. The solar PV system connects to the bus via a DC-to-AC inverter, and the lithium battery system connects to the bus via a bi-directional AC-DC converter. The microgrid system is controlled using a conventional operation strategy to maximize renewable consumption [13]. The operation strategy states that solar PV is the primary energy supply, lithium storage is the secondary supply, and grid electricity is the tertiary supply. The precedence means solar generation will be used first to meet the demand. Any excess generation will be charged into lithium storage. When generation cannot meet the demand, energy from storage will be used. When both generation and storage are not enough, grid electricity will be used to meet the demand. The availability of these three supply sources ensures the demand is met at all times.

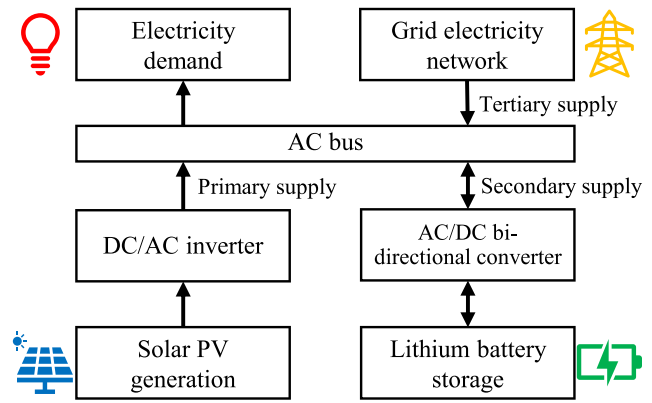


Fig. 9. The domestic property's solar-battery microgrid setup and operation control strategy. The microgrid uses a conventional operation strategy to maximize renewable consumption and minimize electricity grid reliance. The primary supply is used first when available, then the secondary, and then the tertiary. The arrows indicate power flow directions. Note power can be charged to or discharged by lithium battery storage, and storage only charges from surplus solar generation.

The domestic property's roof faces southwest and pitches at a 50° angle; it can accommodate 7 kW of solar PV panels. The solar PV system has a 10% energy loss, mainly due to the DC-to-AC inverter [54]. The solar generation is simulated using Pfenninger and Staffell's method via the Renewables.ninja service [54]. The simulation yields hourly solar generation between 2010 and 2019. Then, the data is averaged to produce an hourly solar generation profile for the typical year, shown in Fig. 10. Solar generation is lower during winter and higher during summer, due to summer's higher solar intensity and duration.

The house has two electricity meters, one for water and space heating, and one for all other energy usages. The water and space heaters only operate between 4:00 am to 2:00 pm and 7:00 pm to 11:00 pm. Since 2010, the meter readings have been recorded once every five days. Elexon demand profiles are used to interpolate the hourly demand between the readings [55]. Elexon's domestic economy profiles are used to interpolate heating demands, and domestic profiles are used to interpolate all other demands. The domestic economy profiles are zeroed during heaters' non-operational hours. The hourly demands between 2010 and 2019 are modeled, and the data are averaged to produce the hourly electricity demand profile for the typical year, shown in Fig. 10. The demand is the highest during winter and lowest during summer, and demand variation is also greater during winter. Note the annual demand is 18 MWh, while the annual generation is 7 MWh.

The lithium battery system is assumed to have a charge and a discharge efficiency of 0.8 [40]. Based on the demand, generation, and storage efficiencies, the unconstrained storage profile is constructed using Eq. (2), as shown in Fig. 11. The overall storage profile decreased between start and end, indicating the total generation is insufficient to support the demand. Lithium battery has a recommended depth of discharge of 80% [52], a C-rating of 1C [53], and a leakage rate of 2% per month [46]. Following the steps outlined in Fig. 2, the iterative sizing method is conducted using a multiplier of 0.1 and a permissible difference limit of 0.01. The storage size converged at 601 kWh, and the constrained storage profile is shown in Fig. 11. The zoomed-in figures show the storage profiles have many small peaks and troughs, which outline the daily charge and discharge experienced by storage. These peaks and troughs produce many critical points, which are fed into the difference matrix for sizing. For simplicity, only the two critical points dictating the storage size are shown in the figure. Their difference in storage level represents the largest cumulative charge experienced by storage.

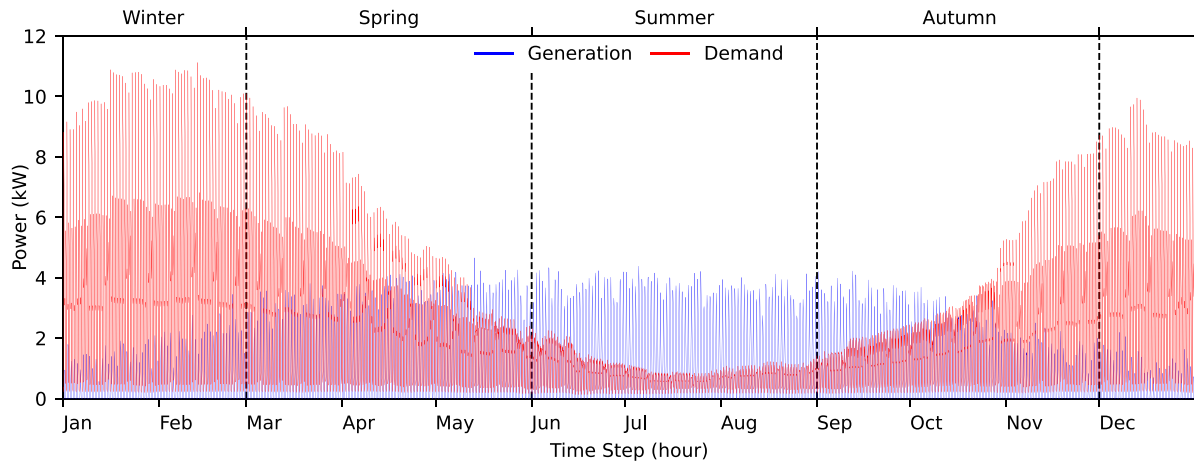


Fig. 10. Solar-battery microgrid's average hourly solar PV generation and electricity demand in a typical year. The dashed lines separate the seasons. The annual demand is 18 MWh, while the annual generation is 7 MWh.

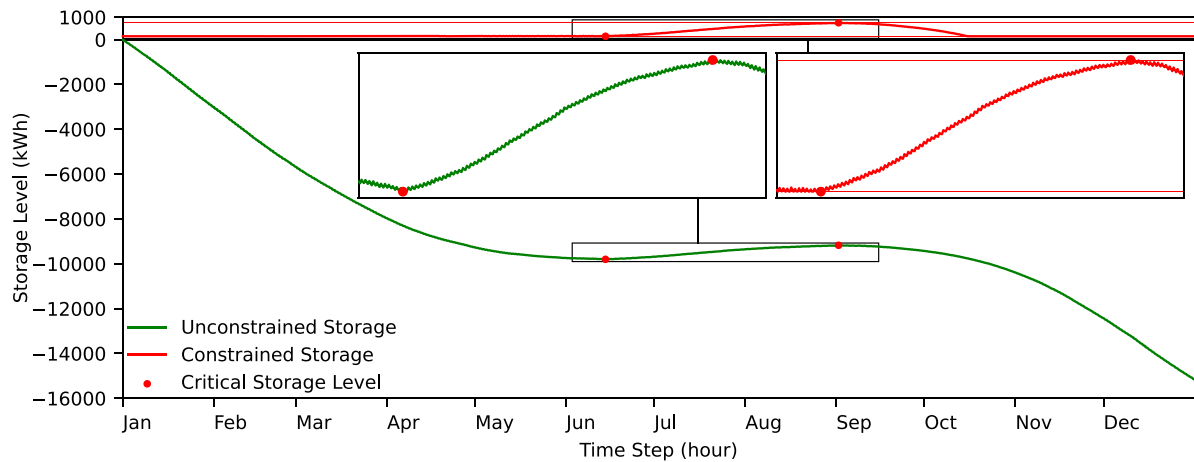


Fig. 11. Solar-battery microgrid's annual constrained and unconstrained storage profiles. The zoomed-in windows show where critical storage levels reside, and their difference is the storage size (601 kWh). The small peaks and troughs in the storage profiles outline the daily charge and discharge experienced by storage. The red horizontal lines mark the upper and lower storage limits, and storage cannot charge beyond the upper limit nor discharge below the lower limit. (For interpretation of the references to color in this figure legend, the reader is referred to the web version of this article.)

The 601 kWh annual storage size is large. To validate this, Monte Carlo simulation is used to see how storage size varies with the uncertainties in demand and generation. Monte Carlo simulation is conducted following the steps outlined in Fig. 3, using historical demand and generation data from 2010 to 2019. The resulting storage size distribution after 3000 simulations is shown in Fig. 12. The result shows that 601 kWh storage size is probable, as it is within one standard deviation from the mean, at the 68th percentile. Note that storage size makes up the 80% depth of discharge, meaning the total storage capacity is 751 kWh, which is beyond the 100th percentile. This means the total storage capacity can maximize renewable consumption even in the worst-case scenario of the Monte Carlo simulation.

The large size is due to the annual design period, which forces the design to account for seasonal storage in addition to daily storage. Seasonal storage is only used once per year; they are charged during summer (June, July, August) and discharged during autumn (September, October), as shown in the constrained storage profile in Fig. 11. In contrast, daily storage is charged during the day and discharged at night, as shown by the small peaks and troughs in the zoomed-in window in Fig. 11. The higher charge and discharge frequency mean the daily storage provides more energy per unit of storage capacity than seasonal storage.

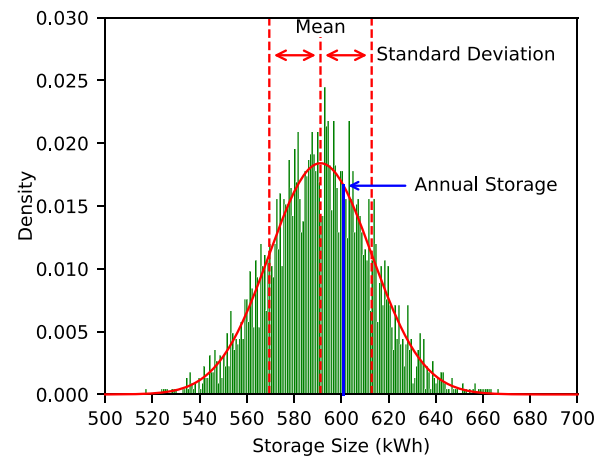


Fig. 12. Histogram of storage size distribution from Monte Carlo simulation. The annual storage size calculated using typical year demand and generation profiles is within one standard deviation from the mean. Note that storage size (601 kWh) constitutes the 80% depth of discharge, meaning the total storage capacity (751 kWh) is beyond the 100th percentile of the storage size distribution.

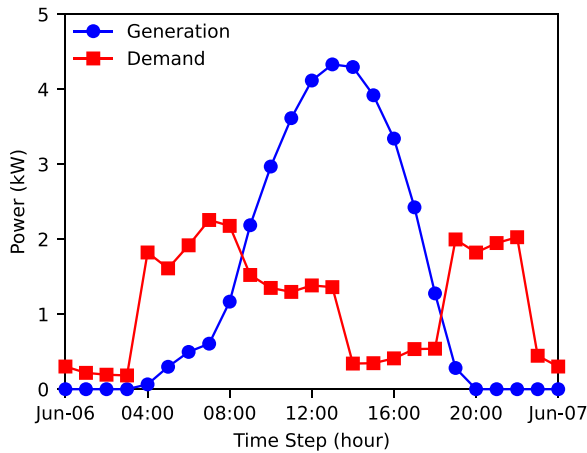


Fig. 13. Solar-battery microgrid's hourly average solar generation and electricity demand on June 6th. This day requires the largest storage due to high surplus generations during the day and high excess demands at night.

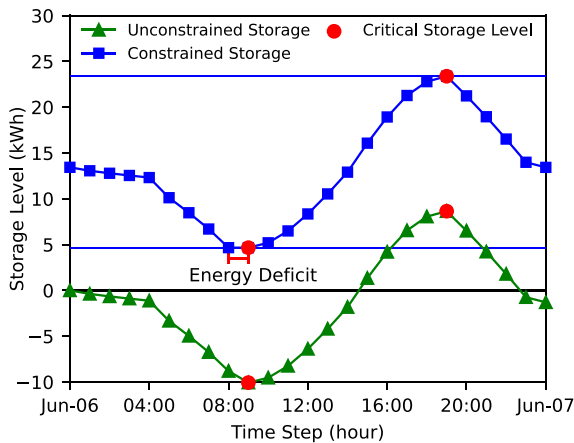


Fig. 14. Solar-battery microgrid's daily design constrained and unconstrained storage profiles on June 6th. This day requires the largest storage size (19 kWh). The blue horizontal lines mark the upper and lower storage limits. The storage cannot discharge below the lower limits, and energy deficits occur when storage cannot discharge to meet the demand. (For interpretation of the references to color in this figure legend, the reader is referred to the web version of this article.)

June 6th requires the largest daily storage size, because it has both high surplus generations and excess demands. The largest daily storage size defines the separation between daily and seasonal storage. The day's hourly generation and demand profiles are shown in Fig. 13. Solar generation only occurs during daylight hours and peaks at noon. The demand is dominated by the heater, which operates between 4:00 am to 2:00 pm and 7:00 pm to 11:00 pm. Other demands follow the typical “duck curve” pattern, where the demand is lowest at night; then rises in the morning as people wake up. The demand then dips during late morning before another rise during lunch time at noon. Then it sinks in the afternoon before peaking in the evening during dinner time. Afterward, the demand drops to the lowest level at night.

The daily design period is considered short-term for lithium batteries; thus, storage leakage is ignored. The constrained and unconstrained profiles are shown in Fig. 14, and the resulting storage size is 19 kWh. The unconstrained storage profile is constructed using Eq. (2). The profile decreased from start to end, indicating generation is unable to fully support the demand, and energy deficits will occur. The constrained profile is obtained following the steps outlined in Fig. 2, and energy deficit does occur between 8:00 am to 9:00 am. The constrained profile

increases during the day as it charges from surplus solar generation, and decreases at night as it discharges to meet the excess demand.

Storage is sized using daily, weekly, and monthly design periods to demonstrate the importance of design period. Storage size for each day, week, and month of the year are calculated; the results are shown in Fig. 15.

In Fig. 15(a), the monthly storage size is the largest in June at 64 kWh, and is the smallest in December at 0.8 kWh. The monthly design yields storage sizes much smaller than the annual design. This is because the annual design considers seasonal and inter-monthly storage, where generation is stored during high-generation months, and released during low-generation months. From the start of the year, winter months have the smallest storage sizes. The small storage size is due to the low solar generations and high winter demands, which means most generations are directly used to meet the demand, leaving little surplus generation to charge the storage. Thus, the storage size is small because it cannot be charged. During the spring months, generation slowly rises while demand falls, creating more surplus generation to charge the storage, and more excess demand that needs storage to discharge. The storage size increase reflects the increasing storage utilization. The summer begins in June. During this month, solar generation peaks due to the summer solstice, while the demand is still high. The high generation and high demand create large surplus generations and excess demands, resulting in the largest storage size requirement. During peak summer in July and August, solar generation is high while demand is low. Most day-time demands are directly met by solar generation, leaving only night-time demands that need storage. Since the summer nightly demand is small, the storage size required to meet that demand is also small. Autumn begins in September. During this month, solar generation remains high while demand is rising. The rising demand creates more excess demands, which require more storage. Thus, the storage size has a small peak during September. In the later autumn months, the rising demand and falling generation mean more generations are directly used to meet the demand, leaving less surplus generation to charge the storage, and causing the storage size to decrease. December has the lowest solar generation due to the winter solstice. The low generation and high demand mean most generations are directly used to meet the demand, leaving little surplus generation to charge the storage. Since storage cannot be charged, the storage size is the smallest in December.

In Fig. 15(b), the weekly storage is the largest in the 24th week at 29 kWh, and is the smallest in the 51st week at 0.1 kWh. Storage size for weekly design is smaller than monthly design, because monthly design accounts for inter-weekly storage. The weekly design exhibits similar patterns as the monthly design. The storage size peaks during early summer and early autumn, is smaller during peak summer, and is the smallest during winter. The 51st week contains the winter solstice with the highest demand and lowest generation, which leaves little surplus generation to charge the storage. Since storage cannot be charged, the storage size is the smallest. On the other hand, the 24th week is one week before the summer solstice. During this week, the demand is still high while generation is peaking, creating more surplus generation and excess demand, and causing the storage size to peak. While in the summer solstice week, the generation is higher, but the demand is lower, which means less storage is needed to meet the smaller excess demands.

In Fig. 15(c), the daily storage size is the largest on June 6th at 19 kWh, and is the smallest for several days in late December at 0 kWh. The daily design is smaller than the weekly and monthly designs because they account for inter-day storage. Daily design exhibits similar patterns as the weekly and monthly design. The storage size peaks on June 6th, with a smaller peak on September 13th at 16 kWh. Both days have high generation and high demand, creating more surplus generations during the day and more excess demands during the night, resulting in larger storage size requirements. On the other hand, storage

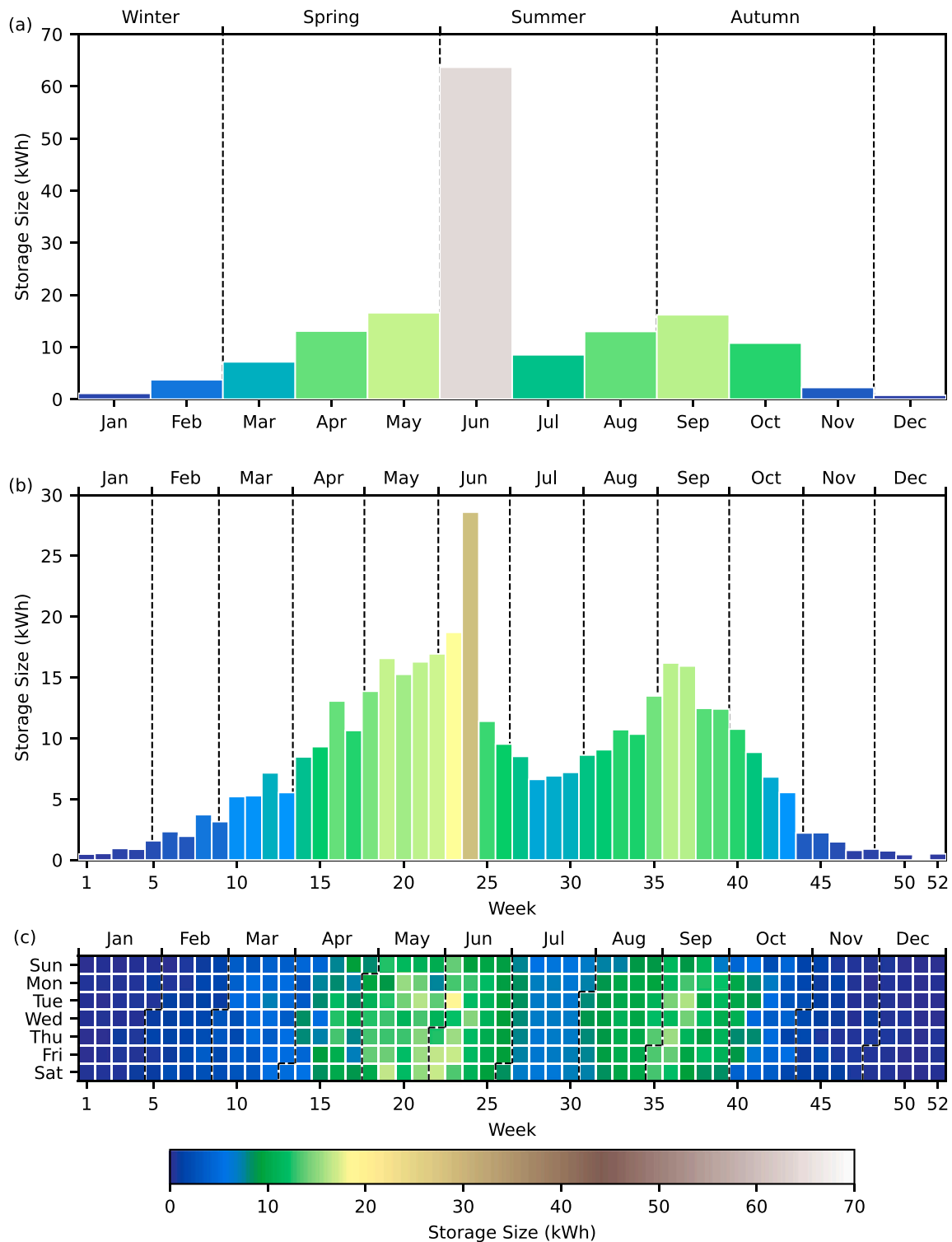


Fig. 15. Storage size calculated using the (a) monthly, (b) weekly, and (c) daily design period. Storage is sized for each month, week, and day of the year. The dashed lines separate the seasons in (a) and the months in (b) and (c). The largest monthly, weekly, and daily storage sizes are 64 kWh, 29 kWh, and 19 kWh, respectively.

is not needed for several days in late December. Late December has the highest demand and lowest generation. All generations are directly used to meet the demand, leaving no surplus generation to charge the storage, resulting in zero storage size.

The patterns exhibited by the daily, weekly, and monthly designs shows storage size is large when generation and demand are high. The high generation and demand create more surplus generations to charge the storage and more excess demands for the storage to meet. With low

generation and high demand, most of the generations are directly used to meet the demands, leaving little surplus generation to charge the storage. Since the storage cannot be charged, the storage size will be small. On the other hand, with high generation and low demand, most of the demands are directly met by generations, leaving little excess demands that need storage; thus, the storage size will also be small. For these reasons, peak summer and peak winter require smaller storage, while early summer and early autumn require larger storage.

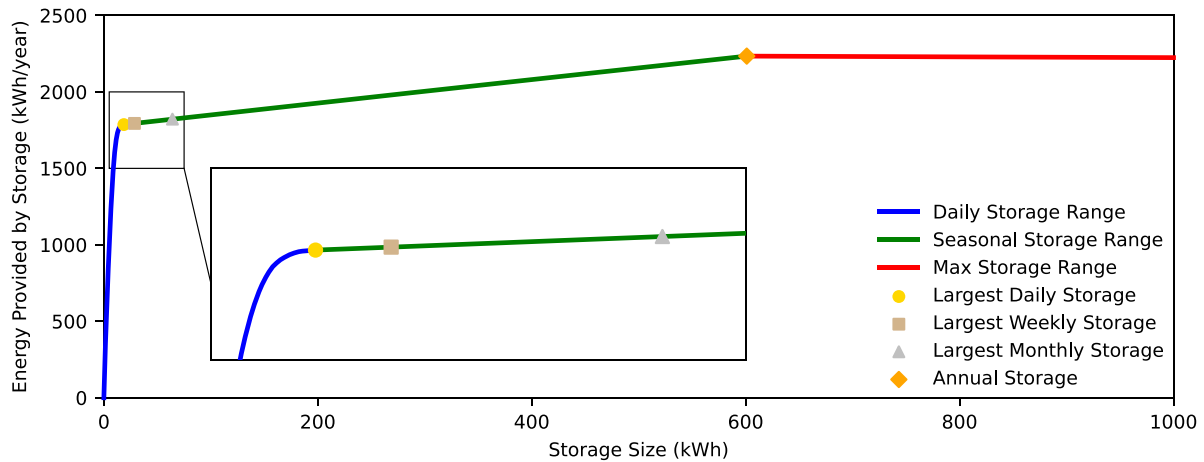


Fig. 16. Storage size and the associated energy provided to the microgrid. The largest daily storage and the annual storage separate the size ranges of daily, seasonal, and max storage. The zoomed-in window shows the largest daily storage separates the daily and seasonal size ranges. At the annual storage size, all the renewable energy that can be stored is stored, and additional storage does not store nor provide more energy. The largest daily design's storage size (19 kWh) is 3% of the annual design's (601 kWh), but provides 80% of the energy (1786 kWh/year) provided by the annual design (2234 kWh/year).

To put the daily, weekly, monthly, and annual designs into perspective, constrained storage profiles for storage sizes ranging from 0 to 1000 kWh are constructed via the enumerative method. The total energy discharged by each storage size is calculated from the constrained storage profiles, which is equivalent to the total energy provided by storage to the microgrid. The results are shown in Fig. 16. The figure shows increasing the storage size has a diminishing return on the additional storage energy provided to the microgrid. The largest daily design and the annual design define the thresholds that separate the figure into three size ranges: daily storage, seasonal storage, and max storage. The daily storage provides the most energy per size unit. Each unit of storage is used for most days during the year; they are charged during the day and discharged at night. Seasonal storage provides much less energy per size unit, because the storage is only used once a year; they are charged during the summer and discharged during autumn. At max storage size, all the energy that can be stored is stored. Additional storage will not provide more energy, and can actually reduce the energy provided, as extra storage induces extra leakage. Note that the data used in this design span a year. If the data span a longer period, the max storage will increase because there will be inter-annual storage, where energy is stored during high-generation years and released during low-generation years. The annual design requires 601 kWh of storage size to provide 2234 kWh of energy per year, while the daily design requires 19 kWh of storage to provide 1786 kWh of energy per year.

Thus, for the presented solar-battery domestic microgrid system operating on a conventional operation strategy, the largest daily design only requires 3% of the storage size of the annual design, but provides 80% of the energy provided by the annual design. Since the microgrid application is on a domestic property, the energy not provided by the daily design is easily supplemented by the electricity grid, while cost-saving from the smaller storage size is significant.

4. Conclusion and future works

The paper presents a novel analytical method to optimally size energy storage. The method is fast, calculates the exact optimal, and handles non-linear models. The method first constructs a temporal storage profile of stored energy, based on how storage charges and discharges in response to generation and demand. The storage is sized according to the largest cumulative charge or discharge in the profile. The method yields the optimal storage size that maximizes storage utilization while eliminating unutilized storage capacity. Maximizing storage utilization also maximizes renewable consumption and minimizes load shedding. The method is applied to two solar-battery

microgrid case studies. The solar-battery microgrids are controlled using a conventional operation strategy, and are physically based in the northern temperate climate zone. Major findings from the case studies are summarized as follows:

- The optimally sized storage does not have wasted storage capacity due to over-sizing, nor cause energy deficits due to under-sizing.
- Energy leakage affects the sizing of long-term storage, and can cause energy deficits in the microgrid system.
- High demand and generation require larger storage, while low demand or low generation requires smaller storage. For these reasons, peak summer and peak winter require smaller storage, while early summer, and early autumn require larger storage.
- Increasing storage size has a diminishing return on the additional storage energy provided to the system. The diminishing return thresholds are defined by the largest daily design and the annual design.
- The largest daily design only requires 3% of the storage size of the annual design, but provides 80% of the energy provided by the annual design.

Three limitations were identified during the testing of the method, and they can be addressed in future works. The first limitation is that with a large number of critical points in the storage profile, the matrix **D** is also large, which slows down the method. Data pre-processing can reduce the number of critical points. For example, signal processing algorithms that filter noise can effectively reduce the number of critical points in the storage profile, while preserving the necessary points for sizing. Thus, future research should look into data pre-processing techniques to speed up the method.

The second limitation is that in scenarios with large leakage and small C-ratings, the method may not yield the storage size that maximizes renewable consumption, as it requires storage wastage. However, the method will yield the closest storage size without wasted capacity. Thus, a potential strategy is to use the proposed method's result as a starting point. Then, use meta-heuristic algorithms, such as particle swarm, to search the nearby region for the storage size that maximizes renewable consumption.

The third limitation is that renewable intermittency can stress the lithium battery, causing the battery's useful life to be shorter than that specified by the manufacturer. Battery degradation is affected by usage, time, temperature, depth of discharge, charge and discharge rates, voltage, and state of charge. The proposed storage sizing algorithm can handle non-linear models. Thus, future research should consider

adopting more accurate and complex lithium battery degradation models with the proposed algorithm, and compare the effects of different degradation models on storage sizing.

CRedit authorship contribution statement

Han Kun Ren: Conceptualization, Methodology, Software, Validation, Formal analysis, Investigation, Writing – original draft, Visualization. **Masaō Ashtine:** Writing – review & editing. **Malcolm McCulloch:** Writing – review & editing, Supervision. **David Wallom:** Conceptualization, Resources, Data curation, Writing – review & editing, Supervision.

Declaration of competing interest

The authors declare that they have no known competing financial interests or personal relationships that could have appeared to influence the work reported in this paper.

Data availability

Data will be made available on request.

Acknowledgments

The author appreciates the financial support provided by Oriel College (University of Oxford) through the Oriel DPhil Scholarship in Engineering Science.

Appendix

The proposed algorithm sizes storage based on the largest cumulative charge or discharge the storage can experience. The cumulative charge or discharge is the difference between critical points in the storage profile. The proof aims to show that all critical point differences

essential for storage sizing are captured by Eq. (5). The proof starts by showing an example storage profile, and lists equations that calculate all critical point differences in the profile. Then, through contradiction and duplication, the proof shows that less than half of the listed equations are essential for storage sizing. These essential equations are captured by the difference matrix **D** in Eq. (5).

Fig. A.1(a) shows an example storage profile with critical points identified. The storage profile is extended to two periods (years) because critical points governing the storage size might be in both periods. Fig. A.1(b) lists the differences between critical points' storage levels. The first row contains the differences between the first critical point's storage level and subsequent points'. The second row contains the differences between the second critical point's storage level and subsequent points'. It continues in this fashion until the last row. The differences are divided into Section A, B, C, D, E, and the following proof shows only differences in Section A and B are essential for storage sizing.

Starting with section C, the following proof shows the first equation in section C duplicates the first equation in section A. Similar proofs can be made for all equations in section C; therefore, section C is not needed.

Proof.

$$\begin{aligned} & S(t'_2) - S(t'_1) \\ &= (S(t_2) + S(T) - S(0)) - (S(t_1) + S(T) - S(0)) \\ &= S(t_2) - S(t_1), \end{aligned}$$

Moving to section D, the following three proofs show the first equation in section D can never be the storage size in all types of storage profiles (increasing, decreasing, and neither). Similar proofs can be made for all equations in section D; therefore, section D is not needed.

Proof. If the overall storage profile is increasing, such that: $S(T) - S(0) > 0$, then storage size is equal to the largest decrease in the profile.

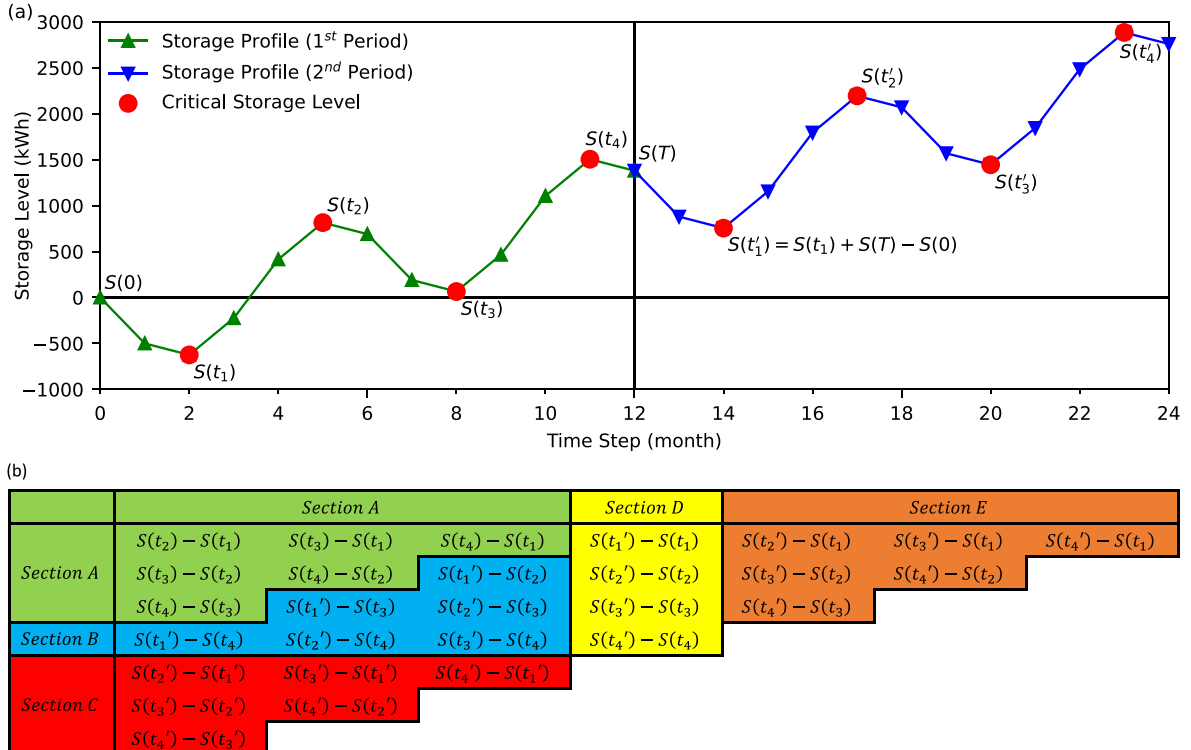


Fig. A.1. Example storage profile's (a) position of critical points and their storage levels, (b) all possible differences between critical points' storage levels. The differences are split into five sections, and the proof will show only Section A and B are essential for storage sizing.

Let $S(t'_1) - S(t_1)$ be the largest decrease, then:

$$\begin{aligned} S(t'_1) - S(t_1) &< 0, \\ (S(t_1) + S(T) - S(0)) - S(t_1) &< 0, \\ S(T) - S(0) &< 0, \end{aligned}$$

Which contradicts the original assumption: $S(T) - S(0) > 0$.

Proof. If the overall storage profile is decreasing, such that: $S(T) - S(0) < 0$, then storage size is equal to the largest increase in the profile. Let $S(t'_1) - S(t_1)$ be the largest increase, then:

$$\begin{aligned} S(t'_1) - S(t_1) &> 0, \\ (S(t_1) + S(T) - S(0)) - S(t_1) &> 0, \\ S(T) - S(0) &> 0, \end{aligned}$$

Which contradicts the original assumption: $S(T) - S(0) < 0$.

Proof. If the overall storage profile is neither increasing nor decreasing, such that: $S(T) - S(0) = 0$, then storage size is equal to the largest change in the profile. Let $S(t'_1) - S(t_1)$ be the largest change, then:

$$\begin{aligned} |S(t'_1) - S(t_1)| &> 0, \\ |(S(t_1) + S(T) - S(0)) - S(t_1)| &> 0, \\ |S(T) - S(0)| &> 0, \end{aligned}$$

Which contradicts the original assumption: $S(T) - S(0) = 0$.

Similarly, the following three proofs show the first equation in section E can never be the storage size in all types of storage profiles (increasing, decreasing, and neither). Similar proofs can be made for all equations in section E; therefore, Section E is not needed.

Proof. If the overall storage profile is increasing, such that: $S(T) - S(0) > 0$, then storage size is equal to the largest decrease in the profile. Let $S(t'_2) - S(t_1)$ be the largest decrease, then:

$$\begin{aligned} S(t'_2) - S(t_1) &< S(t_2) - S(t_1), \\ (S(t_2) + S(T) - S(0)) - S(t_1) &< S(t_2) - S(t_1), \\ S(T) - S(0) &< 0, \end{aligned}$$

Which contradicts the original assumption: $S(T) - S(0) > 0$.

Proof. If the overall storage profile is decreasing, such that: $S(T) - S(0) < 0$, then storage size is equal to the largest increase in the profile. Let $S(t'_1) - S(t_1)$ be the largest increase, then:

$$\begin{aligned} S(t'_2) - S(t_1) &> S(t_2) - S(t_1), \\ (S(t_2) + S(T) - S(0)) - S(t_1) &> S(t_2) - S(t_1), \\ S(T) - S(0) &> 0, \end{aligned}$$

Which contradicts the original assumption: $S(T) - S(0) < 0$.

Proof. If the overall storage profile is neither increasing nor decreasing, such that: $S(T) - S(0) = 0$, then the first equation in Section E is a duplicate of the first equation in Section A:

$$\begin{aligned} S(t'_2) - S(t_1) \\ = (S(t_2) + S(T) - S(0)) - S(t_1) \\ = (S(t_2) + 0) - S(t_1) \\ = S(t_2) - S(t_1). \end{aligned}$$

The proofs show only the critical storage level differences in Section A and B are essential for storage sizing, which are captured by the difference matrix **D** in Eq. (5).

References

- [1] UNFCCC, Adoption of the Paris Agreement, United Nations, 2015, URL https://unfccc.int/sites/default/files/english_paris_agreement.pdf.
- [2] H. Ritchie, M. Poser, Emissions by sector, 2020, URL <https://ourworldindata.org/emissions-by-sector>.
- [3] M. Pehl, A. Arvesen, F. Humpenöder, A. Popp, E.G. Hertwich, G. Luderer, Understanding future emissions from low-carbon power systems by integration of life-cycle assessment and integrated energy modelling, *Nat. Energy* 2 (12) (2017) 939–945.
- [4] IEA, *World Energy Outlook 2020*, Report, International Energy Agency, 2020.
- [5] Y. Yang, S. Bremner, C. Menictas, M. Kay, Battery energy storage system size determination in renewable energy systems: A review, *Renew. Sustain. Energy Rev.* 91 (2018) 109–125, <http://dx.doi.org/10.1016/j.rser.2018.03.047>.
- [6] H. Yang, L. Lu, W. Zhou, A novel optimization sizing model for hybrid solar-wind power generation system, *Sol. Energy* 81 (1) (2007) 76–84, <http://dx.doi.org/10.1016/j.solener.2006.06.010>.
- [7] B.S. Borowy, Z.M. Salameh, Methodology for optimally sizing the combination of a battery bank and PV array in a wind/PV hybrid system, *IEEE Trans. Energy Convers.* 11 (2) (1996) 367–375.
- [8] A.Q. Jakhriani, A.-K. Othman, A.R.H. Rigit, S.R. Samo, S.A. Kamboh, A novel analytical model for optimal sizing of standalone photovoltaic systems, *Energy* 46 (1) (2012) 675–682, <http://dx.doi.org/10.1016/j.energy.2012.05.020>.
- [9] C.V.T. Cabral, D.O. Filho, A.S.A.C. Diniz, J.H. Martins, O.M. Toledo, L.d.V.B. Machado Neto, A stochastic method for stand-alone photovoltaic system sizing, *Sol. Energy* 84 (9) (2010) 1628–1636, <http://dx.doi.org/10.1016/j.solener.2010.06.006>.
- [10] X. Zhu, J. Yan, N. Lu, A probabilistic-based PV and energy storage sizing tool for residential loads, in: 2016 IEEE/PES Transmission and Distribution Conference and Exposition, T&D, IEEE, 2016, pp. 1–5.
- [11] L. Bartolucci, S. Cordiner, V. Mulone, V. Rocco, J.L. Rossi, Hybrid renewable energy systems for renewable integration in microgrids: Influence of sizing on performance, *Energy* 152 (2018) 744–758.
- [12] Y. Zhang, T. Ma, P.E. Campana, Y. Yamaguchi, Y. Dai, A techno-economic sizing method for grid-connected household photovoltaic battery systems, *Appl. Energy* 269 (2020) 115106.
- [13] T. Ma, H. Yang, L. Lu, A feasibility study of a stand-alone hybrid solar-wind-battery system for a remote island, *Appl. Energy* 121 (2014) 149–158, <http://dx.doi.org/10.1016/j.apenergy.2014.01.090>.
- [14] L.M. Halabi, S. Mekhilef, Flexible hybrid renewable energy system design for a typical remote village located in tropical climate, *J. Clean. Prod.* 177 (2018) 908–924, <http://dx.doi.org/10.1016/j.jclepro.2017.12.248>.
- [15] C.K. Das, O. Bass, G. Kothapalli, T.S. Mahmoud, D. Habibi, Overview of energy storage systems in distribution networks: Placement, sizing, operation, and power quality, *Renew. Sustain. Energy Rev.* 91 (2018) 1205–1230, <http://dx.doi.org/10.1016/j.rser.2018.03.068>.
- [16] M.T. Elsir, M.A. Abdulgalil, A.T. Al-Awami, M. Khalid, Sizing and allocation for solar energy storage system considering the cost optimization, in: 2019 8th International Conference on Renewable Energy Research and Applications, ICRERA, IEEE, 2019, pp. 407–412.
- [17] K. Baker, G. Hug, X. Li, Energy storage sizing taking into account forecast uncertainties and receding horizon operation, *IEEE Trans. Sustain. Energy* 8 (1) (2016) 331–340.
- [18] S.X. Chen, H.B. Gooi, M.Q. Wang, Sizing of energy storage for microgrids, *IEEE Trans. Smart Grid* 3 (1) (2012) 142–151, <http://dx.doi.org/10.1109/tsg.2011.2160745>.
- [19] M. Nick, M. Hohmann, R. Cherkaoui, M. Paolone, Optimal location and sizing of distributed storage systems in active distribution networks, in: 2013 IEEE Grenoble Conference, IEEE, 2013, pp. 1–6.
- [20] R. Atia, N. Yamada, Sizing and analysis of renewable energy and battery systems in residential microgrids, *IEEE Trans. Smart Grid* 7 (3) (2016) 1204–1213, <http://dx.doi.org/10.1109/tsg.2016.2519541>.
- [21] L. Al-Ghussain, R. Samu, O. Taylan, M. Fahrioglu, Sizing renewable energy systems with energy storage systems in microgrids for maximum cost-efficient utilization of renewable energy resources, *Sustainable Cities Soc.* 55 (2020) 102059.
- [22] C. Opathella, A. Elkasrawy, A.A. Mohamed, B. Venkatesh, MILP formulation for generation and storage asset sizing and siting for reliability constrained system planning, *Int. J. Electr. Power Energy Syst.* 116 (2020) 105529.
- [23] A.A. Peña, D. Romero-Quete, C.A. Cortes, Sizing and siting of battery energy storage systems: A Colombian case, *J. Mod. Power Syst. Clean Energy* 10 (3) (2021) 700–709.
- [24] M.A. Hannan, M. Faisal, P. Jern Ker, R.A. Begum, Z.Y. Dong, C. Zhang, Review of optimal methods and algorithms for sizing energy storage systems to achieve decarbonization in microgrid applications, *Renew. Sustain. Energy Rev.* 131 (2020) <http://dx.doi.org/10.1016/j.rser.2020.110022>.
- [25] H. Yang, Z. Wei, L. Chengzhi, Optimal design and techno-economic analysis of a hybrid solar-wind power generation system, *Appl. Energy* 86 (2) (2009) 163–169, <http://dx.doi.org/10.1016/j.apenergy.2008.03.008>.

- [26] Y. Zhang, P.E. Campana, A. Lundblad, J. Yan, Comparative study of hydrogen storage and battery storage in grid connected photovoltaic system: Storage sizing and rule-based operation, *Appl. Energy* 201 (2017) 397–411, <http://dx.doi.org/10.1016/j.apenergy.2017.03.123>.
- [27] Y. Zhang, A. Lundblad, P.E. Campana, F. Benavente, J. Yan, Battery sizing and rule-based operation of grid-connected photovoltaic-battery system: A case study in Sweden, *Energy Convers. Manage.* 133 (2017) 249–263, <http://dx.doi.org/10.1016/j.enconman.2016.11.060>.
- [28] M. Shabani, E. Dahlquist, F. Wallin, J. Yan, Techno-economic comparison of optimal design of renewable-battery storage and renewable micro pumped hydro storage power supply systems: A case study in Sweden, *Appl. Energy* 279 (2020) <http://dx.doi.org/10.1016/j.apenergy.2020.115830>.
- [29] C.S. Lai, M.D. McCulloch, Sizing of stand-alone solar PV and storage system with anaerobic digestion biogas power plants, *IEEE Trans. Ind. Electron.* 64 (3) (2017) 2112–2121, <http://dx.doi.org/10.1109/tie.2016.2625781>.
- [30] A. Maleki, M.G. Khajeh, M. Ameri, Optimal sizing of a grid independent hybrid renewable energy system incorporating resource uncertainty, and load uncertainty, *Int. J. Electr. Power Energy Syst.* 83 (2016) 514–524, <http://dx.doi.org/10.1016/j.ijepes.2016.04.008>.
- [31] R.Z. Falama, A.S. Saidi, M.H. Soulouknga, C.B. Salah, A techno-economic comparative study of renewable energy systems based different storage devices, *Energy* 266 (2023) 126411.
- [32] D. Fares, M. Fathi, S. Mekhilef, Performance evaluation of metaheuristic techniques for optimal sizing of a stand-alone hybrid PV/wind/battery system, *Appl. Energy* 305 (2022) 117823.
- [33] A. Ghaffari, A. Askarzadeh, R. Fadaeinedjad, Optimal allocation of energy storage systems, wind turbines and photovoltaic systems in distribution network considering flicker mitigation, *Appl. Energy* 319 (2022) 119253.
- [34] P. Saini, L. Gidwani, An investigation for battery energy storage system installation with renewable energy resources in distribution system by considering residential, commercial and industrial load models, *J. Energy Storage* 45 (2022) 103493.
- [35] B. Yang, J. Wang, Y. Chen, D. Li, C. Zeng, Y. Chen, Z. Guo, H. Shu, X. Zhang, T. Yu, Optimal sizing and placement of energy storage system in power grids: A state-of-the-art one-stop handbook, *J. Energy Storage* 32 (2020) 101814.
- [36] M. Cao, Q. Xu, H. Nazariouya, C.-C. Chu, H.R. Pota, R. Gadh, Engineering energy storage sizing method considering the energy conversion loss on facilitating wind power integration, *IET Gener. Transm. Distrib.* 13 (9) (2019) 1693–1699, <http://dx.doi.org/10.1049/iet-gtd.2018.6358>.
- [37] P. Boonluk, A. Siritatiwat, P. Fuangfoo, S. Khunkitti, Optimal siting and sizing of battery energy storage systems for distribution network of distribution system operators, *Batteries* 6 (4) (2020) <http://dx.doi.org/10.3390/batteries6040056>.
- [38] T. Gu, P. Wang, F. Liang, G. Xie, L. Guo, X.-P. Zhang, F. Shi, Placement and capacity selection of battery energy storage system in the distributed generation integrated distribution network based on improved NSGA-II optimization, *J. Energy Storage* 52 (2022) 104716.
- [39] P.B.L. Neto, O.R. Saavedra, L.A. de Souza Ribeiro, A dual-battery storage bank configuration for isolated microgrids based on renewable sources, *IEEE Trans. Sustain. Energy* 9 (4) (2018) 1618–1626.
- [40] P. Arun, R. Banerjee, S. Bandyopadhyay, Optimum design of diesel generator integrated photovoltaic-battery system, *Energy Fuels* 24 (12) (2010) 6565–6575, <http://dx.doi.org/10.1021/ef101028p>.
- [41] S. Norbu, S. Bandyopadhyay, Power pinch analysis for optimal sizing of renewable-based isolated system with uncertainties, *Energy* 135 (2017) 466–475, <http://dx.doi.org/10.1016/j.energy.2017.06.147>.
- [42] S. Bandyopadhyay, Design and optimization of isolated energy systems through pinch analysis, *Asia Pac. J. Chem. Eng.* 6 (3) (2011) 518–526, <http://dx.doi.org/10.1002/apj.551>.
- [43] Y.F. Nassar, M.J. Abdunnabi, M.N. Sbata, A.A. Hafez, K.A. Amer, A.Y. Ahmed, B. Belgasim, Dynamic analysis and sizing optimization of a pumped hydroelectric storage-integrated hybrid PV/Wind system: A case study, *Energy Convers. Manage.* 229 (2021) 113744.
- [44] S. Kichou, T. Markvart, P. Wolf, S. Silvestre, A. Chouder, A simple and effective methodology for sizing electrical energy storage (EES) systems based on energy balance, *J. Energy Storage* 49 (2022) 104085.
- [45] H.K. Ren, M. McCulloch, D. Wallom, Optimal sizing of solar photovoltaic and lithium battery storage to reduce grid electricity reliance in buildings, in: H. Petran (Ed.), 2022 ECEEE Summer Study, ECEEE, 2022, pp. 1199–1208.
- [46] K. Khan, M.A. Hossain, A. Obaydullah, M. Wadud, PKL electrochemical cell and the Peukert's law, *IJARIE* 4 (2) (2018) 4219–4227.
- [47] I. Hadjipaschalis, A. Poullikkas, V. Efthimiou, Overview of current and future energy storage technologies for electric power applications, *Renew. Sustain. Energy Rev.* 13 (6–7) (2009) 1513–1522, <http://dx.doi.org/10.1016/j.rser.2008.09.028>.
- [48] P. Virtanen, R. Gommers, T.E. Oliphant, M. Haberland, T. Reddy, D. Cournapeau, E. Burovski, P. Peterson, W. Weckesser, J. Bright, SciPy 1.0: fundamental algorithms for scientific computing in Python, *Nature Methods* 17 (3) (2020) 261–272.
- [49] G. Vennam, A. Sahoo, S. Ahmed, A survey on lithium-ion battery internal and external degradation modeling and state of health estimation, *J. Energy Storage* 52 (2022) 104720.
- [50] J. Wang, P. Liu, J. Hicks-Garner, E. Sherman, S. Soukiazian, M. Verbrugge, H. Tataria, J. Musser, P. Finamore, Cycle-life model for graphite-LiFePO₄ cells, *J. Power Sources* 196 (8) (2011) 3942–3948.
- [51] R. Fallahifar, M. Kalantar, Optimal planning of lithium ion battery energy storage for microgrid applications: Considering capacity degradation, *J. Energy Storage* 57 (2023) 106103.
- [52] G. Albright, J. Edie, S. Al-Hallaj, A Comparison of Lead Acid to Lithium-Ion in Stationary Storage Applications, AllCell Technologies LLC, 2012, Published.
- [53] E.C. Castillo, Standards for electric vehicle batteries and associated testing procedures, in: *Advances in Battery Technologies for Electric Vehicles*, Elsevier, 2015, pp. 469–494.
- [54] S. Pfenninger, I. Staffell, Long-term patterns of European PV output using 30 years of validated hourly reanalysis and satellite data, *Energy* 114 (2016) 1251–1265, <http://dx.doi.org/10.1016/j.energy.2016.08.060>.
- [55] Elexon, Load Profiles and their use in Electricity Settlement, Report, Elexon, 2018.